Long-range synchrony between medial prefrontal cortex, thalamus and hippocampus underlies working memory behavior in mice.

Pia-Kelsey O'Neill

Submitted in partial fulfillment of the

requirements for the degree of

Doctor of Philosophy

under the Executive Committee

of the Graduate School of Arts and Sciences

COLUMBIA UNIVERSITY

2013

ABSTRACT

Long-range synchrony between medial prefrontal cortex, thalamus and hippocampus underlies working memory behavior in mice.

Pia-Kelsey O'Neill

Presently, there are no antipsychotic drugs capable of treating the cognitive dysfunctions of schizophrenia. In order to inform the development of better therapies, it is essential to understand the mechanism behind dysfunctional cognition, which requires an understanding of functional cognition. Spatial working memory, a measure of cognitive function, can be assessed in the mouse using a task of delayed alternation: the T-maze. In this thesis, I focus on spatial working memory behavior in the mouse and three brain regions that are implicated in this behavior: the medial prefrontal cortex (mPFC), the hippocampus (HPC) and the medial dorsal thalamus (MD). Lesion and electrophysiological studies in each structure have demonstrated their importance during working memory behavior. Disconnection studies also show that the coordination between the mPFC and either the HPC or MD is important for the behavior, but little is known about the mechanism by which they coordinate. The MD and the ventral region of the hippocampus (vHPC) have robust projections into the mPFC. They are therefore in a good position to influence mPFC activity. Previous reports show that the mPFC and the dorsal region of the hippocampus (dHPC) synchronize activity in the theta range (4-12 Hz) with working memory demand. However, the dHPC does not directly connect with the mPFC so it is unclear

how this coordination occurs. We hypothesized that the vHPC may also be involved in spatial working memory behavior and that it may mediate the dHPC-mPFC theta synchrony observed. To test these hypotheses, we recorded neural activity simultaneously from the mPFC, dHPC and vHPC in mice performing the T-maze task. Local field potential oscillations (LFPs), thought to be a measure of synchronized synaptic activity, were obtained from each area. We observed an increase in theta synchrony between the mPFC and both the dHPC and vHPC. Removing the influence of vHPC both analytically and experimentally, we found a decrease in synchrony of the dHPC-mPFC.

Aside from the disconnection studies, little is known about the MD-mPFC pathway in rodents. However, due to evidence from schizophrenia patients of altered correlation specifically between the MD and PFC, we hypothesized that an electrophysiological correlate of working memory exists in the MD-mPFC pathway as well and that a decrease in MD activity may lead to prefrontal dysfunction. To test these hypotheses, we recorded LFPs from the mPFC and both single unit activity and LFPs from the MD in mice performing the T-maze task. We observed an increase in phase locking of MD cells to mPFC LFPs in beta (13-30Hz) range during the choice phase of the task. We then utilized a pharmacogenetic technique to decrease firing rate in a small portion of MD cells, which resulted in a deficit in both task acquisition and performance. The increase in MD-mPFC beta phase locking we had observed was not present in MD-inactivated animals. Interestingly, beta coherence between the two structures across learning was highly correlated with choice accuracy on the task. This suggests that MD-PFC coordination is predictive of working memory performance.

These findings illustrate how long-range synchrony of the mPFC with HPC in the theta frequency range and with the MD in the beta frequency range may be important markers for normal working memory behavior and if disrupted in humans, could contribute to the cognitive symptoms of schizophrenia.

TABLE OF CONTENTS

List of Figures

Acknowledgments

First, I would like to thank Joshua Gordon, my advisor, for accepting me into his lab for a summer rotation despite the fact that I had no prior Matlab knowledge and little experience with electrophysiology. Josh has provided me with constant guidance and encouragement throughout my graduate career. Next, I want to extend my deepest gratitude to both Torfi Sigurdsson and Sebastien Parnaudeau, my close collaborators during the two portions of my thesis. Torfi was very helpful early on when I was learning the techniques in the lab. I was pleased to work on a manuscript with him recently, as it allowed us to keep in touch after he left to start his own lab in Frankfurt. In the last couple years, I have had the pleasure of working with Sebastien, whose dedication to science, I believe, borders on pathology. Many thanks to my committee members: Rene Hen, Holly Moore, Matthew Shapiro and Christoph Kellendonk for advising me along the way, but especially to Christoph for his patience and insight throughout our collaboration on the thalamus project. Finally, I would not have made it through graduate school without the support I received from the Gordon lab members. I don't know what Josh's secret is for attracting such intelligent, warm, and unique people to his lab, but I feel lucky to have been part of this group.

Chapter 1

Introduction

Introduction

1.1 Background

Overview

Schizophrenia is a chronic and disabling brain disorder that affects about one percent of the population worldwide (Perala et al. 2007). Unfortunately, the large variety of symptoms associated with it as well as the lack of a clear etiology makes this illness particularly challenging to understand. The features of schizophrenia have been classified into two diagnostically relevant categories: “positive” symptoms such as abnormal perceptions (hallucinations) and false beliefs (delusions) and “negative” symptoms, such as emotional blunting and decreased motivation (Association 2000). However, it is increasingly recognized that schizophrenia patients commonly exhibit deficits in a third category: cognition. A recent study found that up to 85% of patients experience some degree of cognitive impairment during the course of the disease (Bowie et al. 2006). These symptoms encompass deficits in attention, behavioral flexibility and working memory-the ability to temporarily store relevant information in order to guide behavior (Park et al. 1995; Keefe et al. 1999). Because this basic function may be crucial for more complex processes such as reasoning, planning and spatial processing, working memory deficits have been hypothesized to be a core symptom of schizophrenia that can disrupt the ability of patients to perform simple tasks of daily life such as following a treatment regimen, completing chores, or holding a job (Silver et al. 2003). Despite the evidence that

working memory deficits can precede and accompany the positive and negative symptoms and thus may play a large role in the functional outcome of the disease (Addington and Addington 2000; Green et al. 2000; Liddle 2000), available medication has not been effective in treating these symptoms (Goldberg and Weinberger 1996; Green et al. 2002). This could be due to the lack in understanding of how the normal brain functions during working memory behaviors.

Many lesion, electrophysiological, and imaging studies have highlighted the crucial role of the prefrontal cortex in working memory (Funahashi and Kubota 1994). Understandably, the prevailing hypothesis regarding the working memory deficits in schizophrenia is one of prefrontal cortex dysfunction. To this end, neuroimaging studies have provided evidence of abnormal recruitment of the frontal areas as patients perform working memory tasks (Andreasen et al. 1992; Weinberger and Berman 1996; Barch et al. 2001). Using the same techniques in areas connected to the PFC, several other brain regions such as the medial dorsal thalamus and hippocampus have gained attention in working memory behavior and in the cognitive deficits of schizophrenia (Minzenberg et al. 2009). Further, there is evidence of abnormal co-activation between these structures and the prefrontal cortex (Seidman et al. 1994; Mitelman et al. 2005). Taking these findings into account, working memory deficits, and cognitive deficits in general, are not likely to be limited to a disruption in the circuitry of one brain structure alone, but extends to the abnormal functional connectivity within a larger network of areas.

With human studies as our motivation, we were interested in further characterizing the activity in both the prefrontal-hippocampal and prefrontal-thalamic pathways during a spatial working memory task in mice. Data from rodents regarding the role of each of these areas also implicates them in working memory behavior (though most literature focuses on the hippocampus) (Floresco et al. 1999; Wang and Cai 2006). Lesion studies show that not only is each region necessary for successful performance in a working memory task (Dunnett 1990; Bailey and Mair 2005; Yoon et al. 2008), but the functional connection within each pathway is required (Floresco et al. 1997; Wang and Cai 2006).

In the following sections, we will provide an overview of the literature in this field in order to present our results within a relevant framework. First, we will discuss what working memory means and compare the tasks developed to test it in humans and rodents. Second, we will review the literature supporting the role of the prefrontal cortex in working memory across species. Next, we will discuss the data regarding the role of the hippocampus and medial dorsal thalamus in rodent spatial working memory behavior with an emphasis on studies examining the disconnection between these areas and the prefrontal cortex. Lastly, we will introduce neural oscillations along with the methods we will use in our own experiments to assess synchrony of oscillations between two brain structures. We will concentrate here on activity in the theta and beta frequency ranges, as these are the most relevant to our findings.

Animal models of working memory

A well-known model of working memory by Alan Baddeley and Graham Hitch describes it as "a brain system that provides temporary storage and manipulation of the information necessary for complex cognitive tasks such as language comprehension, learning and reasoning" (Baddeley 1992). This conception delineated two components of working memory, verbal and spatial, that led to the development of behavioral tasks to differentiate the two. As we obviously cannot test the verbal component in rodents, we will focus on spatial working memory here. A simple example of which in humans involves presenting the subject with a set of spatially arranged dots on a visual space (Figure 1.1 *top*). After a delay during which nothing is presented, a circle appears on the screen. The subject must recognize when the circle location matches a pre-delay dot location (a delay-match-to-sample paradigm) or not (a delay-non-match-to-sample paradigm). Classic working memory operations also involve manipulation of information, protection against interference, and updating of information (Linden 2007).

Non-human animals have been useful in localizing working memory capabilities to specific structures in the brain. While a definition of working memory is perhaps less explicit in rodents than in primates, it is clear that they also must rely on some type of memory in order to form stimulus-response associations to guide behavior (Olton 1979). For example, efficient foraging requires rodents to keep track of which areas of their environment have already been visited and which ones have not-an ability that is vital to adaptive behaviors (Haupt et al. 2010). According to Olton, an acceptable working memory task must have a stimulus-response association that is temporary, is sensitive to interference, and must represent temporal order (Olton 1979).

One of the most common tests of working memory in rodents is the delay-non-match-to-sample T-Maze task (Figure 1.1 *bottom*), first used by Tolman in rats (Tolman 1925). This task makes use of a natural tendency for rodents to alternate spatial locations (Montgomery 1952) and attempt to model the delay-non-match-to-sample tasks used in primates. The T-maze consists of two phases: the sample phase and the choice phase. During the sample phase, one arm of the T is blocked off and the rodent must go to the only open arm to retrieve a food reward. In the choice phase, both arms of the T are open but only the opposite arm (relative to the sample phase) is baited. The rodent must 'hold in mind' where it had gone in the sample phase to go to the opposite arm in the choice phase. This task is sensitive to the length of delay period between phases and to interference from previous trials (Pontecorvo 1983; Dudchenko 2001). In addition, the sample locations (left vs. right) are randomized in order for each stimulus-response association to be critical for only one discrete trial.

The role of the prefrontal cortex in working memory

Early observations from humans with frontal lobe damage pointed to this area's critical involvement in higher cognitive functions. Patients exhibited a range of deficits including those of perception and working memory (Milner 1982; Eslinger and Damasio 1985; Freedman and Oscar-Berman 1986). In the last few decades, as methods such as positron emission tomography (PET) and functional magnetic resonance imagining (fMRI) improved, it became more feasible to monitor correlates of neural activity in the intact human frontal cortex during

normal cognition. An increase in PFC activity is observed during performance on working memory tasks (Weinberger and Berman 1996). Further, there is a large body of evidence for both a decrease in PFC volume as well as reduced activation in schizophrenia patients at rest and during working memory tasks (Weinberger et al. 1986; Andreasen et al. 1992; Baare et al. 1999; Perlstein et al. 2001).

Lesion experiments by Jacobsen demonstrated that the frontal lobe in monkeys is necessary for performance on a spatial delayed alternation task such as the one described above (Jacobsen 1935). This was later shown to be specific to the dorsal lateral region (Funahashi et al. 1993; Petrides 1996). Single-unit recordings in this area revealed cells that increase their firing rates with the onset of the stimulus and remain active during the delay period. This persistent activity is thought to encode the mnemonic contingency of the task (Fuster 1973).

In rodents, lesions in the medial prefrontal cortex (mPFC) – particularly the prelimbic region of the ventral mPFC in rats – results in deficits in delayed responses (Harrison and Mair 1996; Floresco et al. 1999) and in acquisition and performance of other spatial working memory tasks (Dalley et al. 2004; Kellendonk et al. 2006). These similarities suggest a functional comparability of the dorsal lateral PFC in primates and the mPFC of rodents.

The prefrontal cortex in a larger circuit for working memory

The PFC is a site of multimodal convergence for several brain structures. It in interconnected with most sensory and motor systems within the cortex as well as many subcortical structures in the limbic and basal ganglia pathways. Unsurprisingly, several other regions of the brain have been implicated in working memory: the parietal cortex, anterior cingulate, basal ganglia, hippocampus and thalamus (Jonides et al. 1993). In addition, schizophrenia patients exhibit decreased volume in the thalamus, hippocampus and basal ganglia as well as the PFC (Heckers 1997). Furthermore, imaging studies in schizophrenia patients reveal decreased activation of the medial dorsal nucleus of the thalamus and the medial temporal lobe during a variety of tasks of executive function (Andrews et al. 2006; Minzenberg et al. 2009; Luck et al. 2010).

A disconnection hypothesis of schizophrenia suggests that the symptoms are produced by a disruption of coordination between brain regions. The structural abnormalities in this view are secondary to aberrant functional interactions (Friston 1998). In line with this, a meta-analysis of diffusion tensor imaging studies in schizophrenia patients has shown significant volume reduction in two main tracts, the PFC to the temporal lobe containing the hippocampus and the PFC to the thalamus and cingulate cortex (Ellison-Wright and Bullmore 2009)

The prelimbic mPFC of rodents has widespread anatomical connections. A non-exhaustive list of its projections includes the striatum, the basolateral amygdala, the medial dorsal and other midline thalamic nuclei, and the ventral tegmental area (Sesack et al. 1989). It receives input mainly from other prefrontal areas, the ventral hippocampus and subiculum, the medial dorsal thalamus, and the basal amygdala (Hoover and Vertes 2007). While several of these areas most

likely play a role in mPFC function, we will focus on the two major inputs that are also consistently implicated in spatial working memory in mice: the HPC and the MDth.

Hippocampal-prefrontal cortex pathway in rodent working memory

Like the mPFC, the hippocampus is also critically involved in spatial working memory in rodents (Kesner et al. 1996; Hampson et al. 1999; Lee and Kesner 2003). Inactivation or lesion to the CA1 region produces a severe deficit in spatial working memory (Hampson et al. 1999; Yoon et al. 2008). Further, several studies demonstrate the role of communication between the HPC and mPFC in the radial arm maze (Floresco et al. 1997; Izaki et al. 2008) and the T-maze (Wang and Cai 2006). In Wang et al., the experimenters took advantage of the fact that HPC to mPFC projections are ipsilateral and performed a "disconnection" between the two areas. They showed that a unilateral hippocampal inactivation combined with an ipsilateral mPFC inactivation has no effect on behavior in the T-maze task, but that inactivation of the HPC on one side and the mPFC on the contralateral side leads to more errors. Thus, it is the functional connection between these two regions that is necessary for successful navigation in the maze.

Medial dorsal thalamus-prefrontal cortex pathway in rodent working memory

The prefrontal region in rodents is defined in large part based on a dense projection from the MD (Jones 2007). Midline thalamic inputs have been hypothesized to play a role in the processes of arousal and attention (Van der Werf et al. 2002) and/or to gate flow of

information to limbic forebrain (Vertes 2006; Vertes et al. 2006). The function of the MD in working memory per se is debated. Many groups have reported impairment in working memory in MD lesioned rats (Stokes and Best 1990; Hunt and Aggleton 1998; Floresco et al. 1999; Bailey and Mair 2005) but several other studies did not observe such effects (Beracochea et al. 1989; Hunt and Aggleton 1991; Neave et al. 1993)

In a study similar to the HPC-mPFC disconnection experiments, a disconnection between the MD and mPFC was probed in rats to establish the importance of functional connectivity of this pathway during working memory. In this study, a unilateral lidocaine inactivation of the MD and a contralateral, but not ipsilateral, inactivation of the mPFC resulted in more deficits on a working memory task (Floresco et al. 1999).

While these demonstrations of the importance of functional connectivity in the mPFC-HPC and MD-mPFC support the disconnection hypothesis in schizophrenia, the mechanism by which these structures coordinate during cognitive processes is not well understood. A useful tool for studying long-range connectivity between neural networks is to record the ongoing oscillations in activity within them (Buzsaki 2004). Oscillations from two areas can then be analyzed to reveal the dynamic patterns of synchrony within the brain as an animal navigates through its environment.

Oscillations and working memory

A prominent property of neural networks is their tendency to participate in oscillatory activity. Oscillations arise from the synchronous, phasic activation of a population of neurons within a region of brain tissue, which results in a repetitive rise and fall of the extracellular electric potential. These fluctuations in voltage can be recorded at various spatial levels, termed the encephalogram (EEG) or magneto encephalogram (MEG) when recorded from the scalp usually in humans and the local field potential (LFP) when recording from an electrode placed within the brain usually in monkeys and rodents (Buzsaki et al. 2012).

Oscillations are categorized into different frequency bands: delta (1-3Hz), theta (4-8Hz), alpha (8-12Hz), beta (13-30Hz) and gamma (40-200Hz). In rodents, there is no distinction between theta and alpha bands and the two are merged into a 4-12Hz 'theta' band. On a functional level, working memory in primates and rodents has been reflected across all frequencies, but most often associated with theta. Theta band energy can be detected in humans by both MEG and EEG methods and is evident during working memory tasks (Gevins et al. 1997; Sarnthein et al. 1998; Klimesch 1999; Tesche and Karhu 2000). Activity in the beta range has also been implicated in cognitive tasks that involve sensory gating and reward evaluation (Kisley and Cornwell 2006; Marco-Pallares et al. 2008) but little is known of the relevance for working memory (but see (Siegel et al. 2009).

There is growing evidence for the role of oscillations and synchrony in the psychopathology of schizophrenia. Several EEG and MEG studies have shown that oscillations of different frequencies within and between brain regions are altered at rest (Boutros et al. 2008) and

during cognitive tasks (Ford et al. 2002; Schmiedt et al. 2005; Haenschel et al. 2007). For example, in a study by Schmiedt et al, 2005, normal and schizophrenia patients were tested on a working memory task. While evoked theta band activity increased in the frontal area of normal subjects, no increase was observed in patients who performed more poorly on the task.

In rodents, the majority of reports focus on theta (4-12Hz) and gamma (40-200Hz) oscillations of the hippocampal system, as these are quite prominent in neural recordings. Theta frequency oscillations depend on ongoing behavior in rats (Grastyan et al. 1959; Vanderwolf 1969) and are most pronounced during REM sleep (Jouvet 1969)and during voluntary/exploratory activities (Vanderwolf 1969)

Neuronal oscillations synchronize across brain regions

Communication between brain areas is reflected in patterns of synchronization and desynchronization of oscillations over time (Singer 1999; Varela et al. 2001). Rhythmic modulations of neural excitability can affect the likelihood of spike output and also the sensitivity to spike input (Fries 2005). Synchrony or coordination of neuronal discharge could thus be a mechanism to bind distributed sets of neurons into coherent networks that represent the neural correlate of cognitive significance. The first synchronous oscillations to have a proposed role were in the gamma range, as described by Gray and Singer in feature binding in cat V1 (Gray and Singer 1989). The particular frequency of synchronous firing might highlight spatially separable neural populations belonging to the same functional network. One

population of neurons could therefore participate in multiple, specific processes with other populations, depending on the dominant frequency of oscillation.

In rodents, the ability to record LFPs from within the brain allows collection of activity from subcortical structures, an advantage over EEG and MEG recordings. The subsequent analysis of synchrony is then more localized to the region of interest. In this thesis, we will assess the synchrony of LFPs from two brain regions using three different methods: correlations in power, coherence of phase and power fluctuations and phase locking of single cells to LFPs. Power correlations compare the amplitude of the LFPs from two areas while coherence involves comparing both amplitude and phase relationship of LFPs over time. If the LFPs in a given frequency range have a consistent relationship, they are 'coherent' at that frequency. Phase locking measures the degree to which a given cell in one region fires at a specific phase of the LFP from the other region.

Functional connectivity in the mPFC-HPC pathway during working memory

In the case of hippocampal-prefrontal interactions, theta frequency (4-12 Hz) oscillations are thought to play a particularly important role (Benchenane et al. 2010; Colgin 2011; Gordon 2011). The firing of mPFC neurons is modulated by the phase of theta oscillations in the hippocampus, and the LFPs in the two structures display coherence in the theta frequency range (Jones and Wilson 2005; Siapas et al. 2005; Sirota et al. 2008; Benchenane et al. 2010; Hyman et al. 2010; Sigurdsson et al. 2010). Furthermore, neural activity in the mPFC becomes

synchronized with activity in the hippocampus during spatial working memory tasks and the strength of this synchrony correlates with an animal's behavioral performance (Jones and Wilson 2005; Hyman et al. 2010; Sigurdsson et al. 2010). Reduction in phase locking between mPFC spikes and HPC theta LFP are predictive of errors, which suggests that mPFC-HPC synchrony is either necessary for correct retrieval or reflects decision confidence (Jones and Wilson 2005).

An oversight in the studies above is that they focus mainly on one area of the hippocampal extent: the dorsal sub region, which does not project to the mPFC. This focus does not address the role of the ventral CA1/subiculum, which has a dense, monosynaptic projection to the prelimbic (PL) and infralimbic (IL) region of the mPFC. While there is less evidence of vHPC role in spatial working memory, both the dorsal and ventral HPC regions seem to encode spatial information through the formation of place fields (Wilson and McNaughton 1993). In addition, a tetanic stimulation of vHPC-PL pathway induces long-term potentiation in the PL (Laroche et al. 1990). Therefore, because anatomy is not divorced from function, we will examine if and how the vHPC-mPFC pathway is modulated by a T-maze task and determine its role in mediating observed dHPC-mPFC synchrony.

Functional connectivity in the mPFC-HPC pathway during working memory

Electrophysiological evidence of the role of MDth-mPFC synchrony during working memory is nonexistent. Based on the evidence from lesion studies in rodents, imaging studies in

schizophrenia, and its anatomical connection to the PFC across species, we hypothesized the MDth plays a key role in mPFC function. We will therefore examine if and how the MD-mPFC pathway is modulated by a T-maze task and determine its role in MD-mPFC synchrony.

1.2 Approach

As reviewed above, the functional outcome of schizophrenia is related to the severity of the associated cognitive symptoms. Of these, working memory may be a core feature of schizophrenia that supports higher cognitive function. Lesion studies in monkeys and rodents and imaging studies in humans have pointed to the involvement of several structures for successful working memory behavior-the most studied being the prefrontal cortex in primates. However, the mechanism that coordinates the PFC with other areas is still poorly understood. In order to understand the functional coordination of multiple brain regions during working memory behavior we will focus on anatomically connected regions in the mouse and record multi site activity as the mice navigate the T-maze spatial working memory task.

In Chapter 2, we examine the role of the vHPC in working memory and its role in dHPC-mPFC theta synchrony. Previous electrophysiology studies exploring the mPFC-HPC pathway in working memory focused on the dorsal sub region of the HPC though it does not directly project to the mPFC. We hypothesized that because the vHPC has robust axonal projections into the mPFC and is also connected to the dHPC, then we should observe modulation of the vHPC by the same working memory task. We implanted mice with single electrodes in the

mPFC, dHPC and vHPC and recorded LFPs from each region while the animals performed in the T-maze. We found that, like the mPFC and dHPC, theta coherence also increases between the mPFC and vHPC during the choice phase of the task, the phase with the highest mnemonic demand. In addition, using partial correlation analysis to remove the influence of vHPC on dHPC-mPFC synchrony or inactivating the vHPC with muscimol, we were able to disrupt dHPC-mPFC theta coherence.

While there was previously existing evidence on the mPFC-HPC circuit, albeit the focus on the dorsal region, there was little evidence on the role of another major input to the mPFC: the MD thalamus. Many lesion studies in rodents did not agree as to whether the MD had a role in spatial working memory. But, human imaging studies pointed to the MD as one of several regions involved in working memory and several other cognitive processes. Notably, in schizophrenia patients who exhibit working memory deficits, activity in the MD and in the PFC-MD pathway is abnormal.

In Chapter 3, we explore the role of the MD in spatial working memory and its role in mPFC-thalamic synchrony. We implanted mice with high impedance stereotrode wires (to record from single units) in the MD and single electrodes in the mPFC (and for comparison, the dHPC) to record LFPs, and then trained the animals on the same T-maze task used in Chapter 2. We observed an increase phase locking of MD cells to mPFC beta oscillations during the choice phase of the task. To test the requirement of the MD for functional working memory, we then utilized a pharmaco-genetic technique to decrease the firing rate in a small population of MD

cells. This subtle inactivation was sufficient to impair acquisition and performance in the T-maze task. Interestingly, we also no longer observed modulation of activity in the MD-mPFC pathway during the task. Lastly, Chapter 4 will be a discussion of how these areas may interact with each other at different frequencies as well as how other structures may coordinate with the mPFC during working memory.

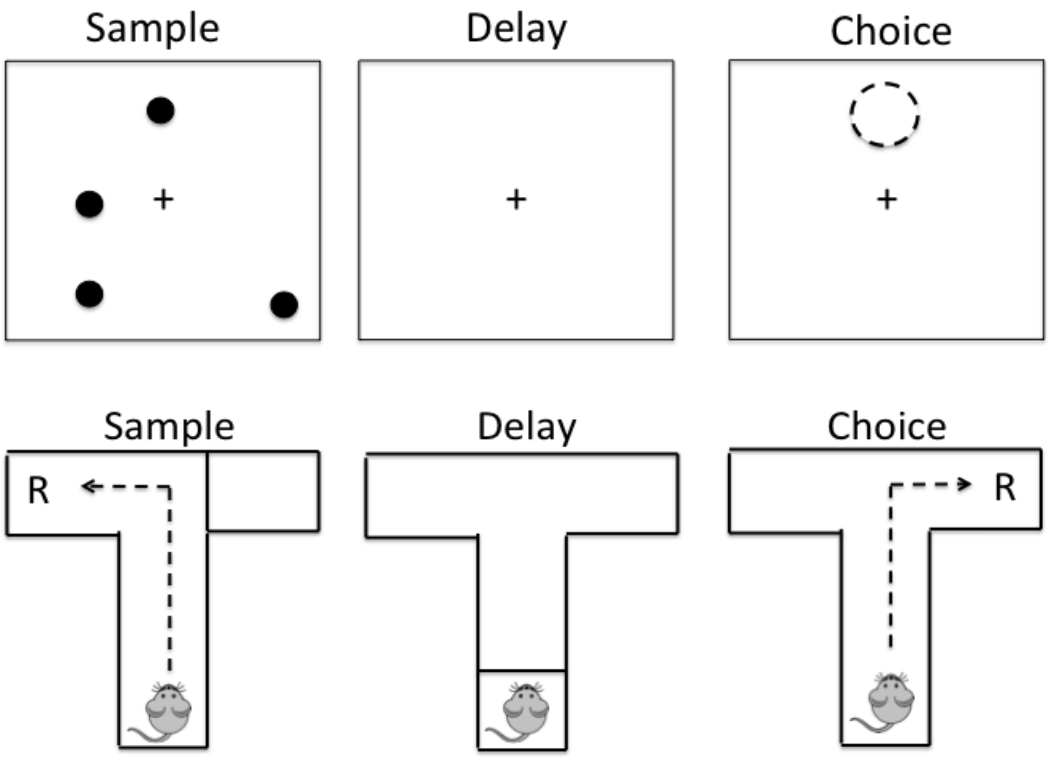

Figure 1.1 Tasks of Spatial working memory in humans (top) and rodents (bottom).

Chapter 2

Inhibition of ventral hippocampus disrupts hippocampal-frontal connectivity

CHAPTER 2: INHIBITION OF VENTRAL HIPPOCAMPUS DISRUPTS HIPPOCAMPAL FRONTAL CONNECTIVITY

(Note: These experiments were completed in collaboration of Torfi Sigurdsson, Ph.D., when he was a post-doctoral fellow in the lab of Joshua Gordon, M.D., Ph.D., in the Psychiatry Department at Columbia University.)

2.1 Introduction

The medial prefrontal cortex (mPFC) and hippocampus are both required for spatial working memory in rodents. Synchronization of theta-frequency oscillations in these structures is thought to be a mechanism for their functional connectivity. However, little is known about oscillations within the mPFC itself, where mPFC theta oscillations might originate, and how they are paced. The dorsal sub region of the hippocampus (dHPC), on which most studies of dHPC-mPFC synchrony focus, does not project directly to the mPFC. Therefore it is unclear how the dorsal hippocampus could influence oscillations in the mPFC. The ventral hippocampus (vHPC) does send robust axonal projections to the mPFC and could potentially mediate the synchrony observed between mPFC and dHPC. To examine these issues, we recorded simultaneously from the dHPC, vHPC and mPFC in mice performing a spatial working memory task. We found that vHPC theta oscillations share similar peak frequency and amplitude with the mPFC and, like those in the dHPC, synchronize with the mPFC during the task. Removing its influence either computationally (through partial correlation analysis) or experimentally (through pharmacological blockade with muscimol) decreases measures of synchrony between the mPFC

and dHPC. These data demonstrate that theta-frequency synchrony between the mPFC and dHPC is mediated, at least in part, through the vHPC.

2.2 Results

Theta oscillations in the ventral but not the dorsal hippocampus are modulated during spatial working memory

A major source of inputs to the mPFC comes from the hippocampus, which is known to generate robust theta oscillations (Buzsaki 2002). Although most previous studies have focused on theta oscillations in the dorsal hippocampus (dHPC), this sub region of the hippocampus only projects indirectly to the mPFC. However, the ventral hippocampus (vHPC) gives rise to monosynaptic excitatory projections to the mPFC (Degenetais et al. 2003; Hoover and Vertes 2007). We therefore asked how theta oscillations in the vHPC and dHPC compare to those in the mPFC and whether they are also modulated by the spatial working memory task. Theta oscillations in the dHPC were both larger in amplitude and of a higher frequency than in either the vHPC or mPFC (Figure 2.1A,B; $p<0.01$, Wilcoxon signed-rank test), consistent with similar observations under other behavioral conditions (Adhikari et al. 2010; Royer et al. 2010). However, theta oscillations did not differ between the vHPC or mPFC in terms of either power or frequency ($p>0.05$, Wilcoxon signed-rank test). Furthermore, we found that theta oscillations in the vHPC, but not the dHPC, increased in strength during the choice phase (Figure 2.1C,D). Thus, theta oscillations in the vHPC resemble mPFC theta oscillations, both qualitatively and in

terms of their modulation by the spatial working memory task, possibly reflecting the direct connections between the two areas.

Both sub regions of the hippocampus synchronize with the medial prefrontal cortex during working memory

These results raise the possibility that theta oscillations in the mPFC, and their modulation by spatial working memory, might be driven by theta activity in the hippocampus, perhaps via the vHPC. If so, one would expect theta-frequency synchrony between both hippocampal sub regions and the mPFC to be modulated by the spatial working memory task. To address this issue, we measured both coherence and power correlations between the mPFC and both vHPC and dHPC. As shown in Figure 2.2A and B, LFPs in both the dHPC and vHPC were coherent with the mPFC in the theta-frequency range, and the magnitude of theta coherence increased during the choice phase ($p<0.01$, Wilcoxon signed-rank test). In contrast, theta coherence between the two hippocampal sub regions did not increase during the choice phase ($p>0.05$, Wilcoxon signed-rank test). Similar results were obtained when synchrony was measured by correlating theta-frequency power in the three structures (Figure 2.2C,D, $p<0.05$, Wilcoxon signed-rank test).

The ventral hippocampus mediates hippocampal-prefrontal theta synchrony

Although both the dHPC and vHPC display theta synchrony with the mPFC, only the vHPC projects directly to the mPFC, allowing for the possibility that hippocampal-mPFC theta synchrony is mediated by the vHPC. Consistent with this, we found that periods of high dHPC-mPFC theta coherence were associated with high dHPC-vHPC theta coherence (Figure 2.3A, B), suggesting the possibility that in order for the dHPC to synchronize with the mPFC, it must also synchronize with the vHPC. Notably, vHPC-mPFC coherence was less correlated with vHPC-dHPC coherence ($p<0.01$, Wilcoxon sign-rank test, Figure 3B), suggesting that the ability of the vHPC to synchronize with the mPFC did not depend on its ability to synchronize with the dHPC. In order to further assess the contribution of vHPC to hippocampal-prefrontal synchrony, we calculated partial correlations between dHPC and mPFC theta power, taking into account their correlations with the vHPC (Figure 2.3C, left). When compared to the simple correlation (i.e. without taking into account the effects of vHPC activity), the partial correlation of dHPC and mPFC theta power was significantly lower ($p=0.01$; Wilcoxon signed-rank test). Importantly, however, the vHPC-mPFC theta power partial correlation (i.e. taking into account activity in dHPC) was not significantly different from its simple correlation (Figure 2.3C, right; $p>0.05$; Wilcoxon signed-rank test). We also re-examined the modulation of hippocampal-prefrontal synchrony by spatial working memory using the partial correlation method. This revealed that dHPC-mPFC theta power correlations did not increase in the choice phase when vHPC activity was taken into account ($p>0.05$; Wilcoxon signed-rank test), whereas the increase in vHPC-mPFC power correlations remained significant after taking into account dHPC activity ($p<0.05$; Wilcoxon signed-rank test).

Taken together, these results support the hypothesis that hippocampal-prefrontal theta synchrony is primarily mediated by the vHPC. This hypothesis predicts that inactivating the vHPC should disrupt hippocampal-prefrontal synchrony. To test this prediction, we recorded LFPs from the mPFC, dHPC and vHPC before and after infusion of the $GABA_A$ receptor agonist muscimol into the vHPC (see methods). As an initial test of the action and time course of muscimol, we injected one animal with muscimol in the vHPC and observed a decrease in dHPC-mPFC coherence approximately 16 minutes after infusion (Figure 2.4A). We then performed a controlled experiment to compare dHPC-mPFC coherence after infusion of saline and muscimol. We found that vHPC inactivation decreased dHPC-mPFC theta coherence (Figure 2.4B, D; $p=0.01$, Wilcoxon sign-rank test), confirming the role of vHPC in hippocampal-prefrontal synchrony. To control for possible effects of multiple injections, we also injected saline twice into the vHPC. This, however, had no effect on hippocampal-prefrontal synchrony (Figure 2.4C,E; $p>0.05$). As we had implanted electrodes bilaterally into each region, we were able to assess the effect of unilateral inactivation of the vHPC on dHPC-mPFC coherence on the contralateral side. Due to the ipsilateral connectivity of the hippocampal-prefrontal circuit, this served as an important within-animal control. Importantly, we did not observe a significant change in dHPC-mPFC coherence contralateral to the vHPC where muscimol was infused (Figure 2.4F, $p>.05$, Wilcoxon sign-rank test).

We next examined the effect of vHPC inactivation on oscillations within the three structures (Figure 2.5A). Although vHPC theta power was lower following muscimol infusion, this effect did not reach statistical significance (Figure 2.5B, $p=0.08$, Wilcoxon sign-rank test). However, we did observe a significant decrease in vHPC gamma-frequency (40-60 Hz) power

following muscimol infusions (Figure 2.5A,B $p<0.01$, Wilcoxon sign-rank test), confirming the efficacy of the inactivation. In the dHPC, there was a small but statistically significant decrease in theta power following muscimol infusions but no change in gamma power (Figure 2.5A,C; $p<0.01$ and $p>.05$ for theta and gamma power, respectively, Wilcoxon sign-rank test). We were concerned that the change in hippocampal-prefrontal synchrony following vHPC inactivation could be secondary to the decrease in dHPC theta power. We therefore asked whether the effects of muscimol on dHPC-mPFC coherence were correlated with its effects on dHPC theta power. However, we found no evidence of such a relationship (Pearson's $r = 0124$, $p>0.05$), suggesting that the change in dHPC-mPFC coherence could not be explained by the decrease in dHPC power alone (Figure 2.6). Finally, neither mPFC theta power nor vHPC-mPFC theta coherence decreased significantly following vHPC inactivation (data not shown). This, combined with the lack of a drop in vHPC theta power, suggests that the theta oscillation seen in the vHPC itself is not dependent upon local cellular activity, and/or that our infusion was too small to substantially affect the large theta generator in the HPC. Nonetheless, this subtle manipulation was able to disrupt dHPC-mPFC communication, a clear demonstration of the importance of the vHPC in maintaining dHPC-mPFC coordination.

2.2 Discussion

How do theta oscillations emerge within the mPFC? One possibility is that they reflect rhythmic input from the vHPC, which sends excitatory projections to the mPFC and also displays

robust theta oscillations. However, our finding that mPFC theta power was not affected by inactivating the vHPC argues against this possibility. Nevertheless, it is possible that rhythmic input from other structures is responsible for theta generation in the mPFC. Alternatively, theta oscillations in the mPFC might arise through local mechanisms, for example through the activity of specific subtypes of interneurons (Blatow et al. 2003). The intrinsic membrane properties of mPFC neurons may also enable them to oscillate preferentially in the theta frequency range (Dembrow et al. 2010). Interestingly, a computational model of working memory suggests that short-term synaptic plasticity can generate theta-frequency network dynamics under some conditions (Mongillo et al. 2008). Whether these or other mechanisms underlie theta generation in the mPFC will be important foci for future research.

Given that the hippocampus generates robust theta oscillations (Buzsaki 2002) and is also required for spatial working memory performance, we asked whether hippocampal theta oscillations are modulated by spatial working memory performance. Consistent with previous findings (Jones and Wilson 2005; Montgomery et al. 2009) we found that theta power in the dHPC did not increase during the choice phase. However, we observed a robust increase in vHPC theta power that was comparable to what was observed in the mPFC. Interestingly, theta oscillations in the vHPC, but not the dHPC, also increase during anxiety tasks, in which animals must choose between exploration or safety (Adhikari et al. 2010). The differential modulation observed in these two tasks suggests that theta oscillations in the vHPC are modulated more by behavioral context than theta oscillations in the dHPC, consistent with a body of literature documenting functional differences between the two sub regions (Bannerman et al. 2004; Fanselow and Dong 2010). Furthermore, dHPC theta was qualitatively and quantitatively

different from vHPC theta. As we, and others, have reported (Adhikari et al. 2010; Royer et al. 2010), theta oscillations were of lower magnitude and frequency in the vHPC than in the dHPC. This is unlikely to reflect different recording locations as these differences hold when recordings are restricted to the same hippocampal layers in both dorsal and ventral subdivisions (Adhikari et al. 2010)Supplementary Figure S2). We also found that mPFC theta was more similar to vHPC than to dHPC theta, consistent with the connectivity between the two regions. However, we cannot exclude the possibility that different recording locations within the mPFC might have produced different results. Nevertheless, these results argue against the possibility that theta oscillations in the mPFC are volume conducted from the hippocampus (Sirota et al. 2008). If that were the case, the frequency of mPFC theta would be expected to be more similar to dHPC theta than vHPC, since the dHPC generates stronger theta oscillations and is closer to the mPFC than the vHPC.

Our study also sought to address how mPFC theta oscillations are synchronized with theta oscillations in the hippocampus. Previous studies reported that during spatial working memory tasks, neural activity in mPFC and dHPC becomes synchronized in the theta frequency range, and the degree of synchrony correlates with behavioral performance (Jones and Wilson 2005; Hyman et al. 2010; Sigurdsson et al. 2010). However, because the hippocampal projections to the mPFC originate in the ventral but not the dorsal HPC (Hoover and Vertes 2007), it is unclear how theta oscillations in the dHPC and mPFC can become synchronized. One possibility is that this is mediated by the vHPC, which is connected to the dHPC and also projects directly to the mPFC (Degenetais et al. 2003; Hoover and Vertes 2007). Our findings are in agreement with such a possibility. First, we observed that dHPC-mPFC and dHPC- vHPC theta coherence was

positively correlated. Second, analytically removing the influence of vHPC activity (using partial correlations) dramatically reduced the magnitude of dHPC-mPFC theta power correlations, whereas removing the influence of dHPC did not affect vHPC-mPFC theta power correlations. Finally, pharmacologically inactivating the vHPC decreased theta synchrony between dHPC and mPFC. These results are consistent with either a permissive role for the vHPC, in which its efferent to the mPFC *support* hippocampal-prefrontal synchrony, or a direct role in which information flows from the dHPC *through* the vHPC to the mPFC. Further experiments will be required to distinguish between these possibilities.

Our findings suggest that in order for the dHPC to synchronize with the mPFC, it must synchronize with the vHPC as well. They are consistent with the hypothesis that the vHPC acts as a conduit directly facilitating spatial working memory by relaying spatial information from the dHPC to the mPFC. This hypothesis is supported by studies reporting spatial working memory deficits following inactivation of the vHPC (Floresco et al. 1997; Wang and Cai 2006). However, other studies have reported no effect of vHPC inactivation on spatial working memory (Mao and Robinson 1998; McHugh et al. 2008), perhaps pointing to alternate routes by which the hippocampus interacts with the mPFC. One possibility involves the reuniens nucleus of the thalamus, which has been implicated in tasks requiring the mPFC and hippocampus (Dolleman-van der Weel et al. 2009; Hembrook et al. 2012; Loureiro et al. 2012). Furthermore, a small percentage of neurons in the reuniens projects both to the mPFC and hippocampus (Hoover and Vertes 2012; Varela et al. 2013) that could allow direct facilitation of synchrony between the three structures. Regardless of the contributions other regions may have, our results show that the vHPC plays a notable role in prefrontal-hippocampal

coordination. Whether it has an essential function in spatial working memory is an important subject for further research.

2.3 Methods

Animals

Ten male wild-type C57/Bl6 mice (3-6 months old) were used in the study, 3 of which were obtained from Jackson laboratories and 9 of which were bred at Columbia University. Because of missed placements, only 5 C57/Bl6 mice could be used for the analysis of vHPC activity. We therefore added to our data set of vHPC activity 5 mice of the 129Sv/Ev strain. No differences were found between strains. The procedures described here were conducted in accordance with National Institutes of Health regulations and approved by the Columbia University and New York State Psychiatric Institute Institutional Animal Care and Use Committees

Surgical procedures

Animals were initially anaesthetized with ketamine/xylazine, placed in a stereotaxic frame and maintained on isoflurane for the duration of the surgery. Craniotomies were made to allow two tetrodes or five stereotrodes to be implanted in the medial prefrontal cortex (mPFC; 1.7 mm anterior to the bregma, 0.4 mm lateral to the midline and 1.5 mm below the brain surface) and tungsten wires to be placed into the dorsal (1.94 mm posterior to the bregma, 1.5 mm lateral to the midline and 1.4 mm below the brain surface) and ventral (3.16 mm posterior to the bregma, 3.2 mm lateral to the midline and 4.1 mm below the brain surface) sub regions of the

hippocampus. Skull screws overlying the cerebellum and frontal cortex served as ground and reference, respectively. All wires were connected to a 16-channel interface and the mPFC electrodes were anchored to a microdrive that made it possible to advance them along the dorsoventral axis. To verify recording locations, current (50 mA, 10 s) was passed through the electrodes at the end of the experiment. Animals were then perfused, the brains cut on a cryostat and stained for Nissl bodies using cresyl violet.

Behavior

Animals were trained on a discrete non-match-to-sample T-maze test of spatial working memory as described previously (Sigurdsson et al. 2010). Each trial of the task consisted of two phases. In the 'sample phase', mice ran down the center arm of the maze and were directed into one of the goal arms by a barrier that closed off the other arm. After a brief delay (~10s) the mice again ran down the center arm, but now had to choose between two open goal arms ('choice phase'). To obtain a reward, animals were required to enter the goal arm not visited during the sample phase. After two days of habituation to the maze and two days of shaping, animals were given daily training sessions of ten trials until they reached criterion performance, defined as performance of at least seven trials correct per day for three consecutive days. After this criterion had been reached, animals were given daily sessions of 20–25 trials. Although neural data was recorded throughout the experiment, the results presented here are from post-criterion sessions.

Data acquisition

Neural data (field potentials) were acquired using a 16-channel head stage and a Cheetah data acquisition system (Neuralynx). The animal's position in the T-maze was monitored using two light-emitting diodes mounted on the head stage. To extract field potential activity, signals were band-pass filtered between 1 and 1,000 Hz and digitized at 2 kHz. Further analysis of neural and behavioral data was performed using custom written MATLAB scripts (MathWorks)

Field potential analysis

In order to measure coordination of theta activity in the mPFC and the hippocampus we measured both the coherence of the LFPs in the two structures as well as their power correlations. Coherence was computed using the multi-taper method (MATLAB routines provided by K. Harris and G. Buzsaki). Field potentials were divided into 500 ms segments (50 ms overlap) and the Fourier transform of each segment was computed after being multiplied by two orthogonal data tapers. Coherence was then computed by averaging the cross-spectral densities of two field potential signals across data windows and tapers and normalizing to the power spectral densities of each signal. In order to compute coherence over time, cross-spectral densities were averaged across 10 data windows (overlap 6 windows). Theta coherence was always defined as average coherence between 4 and 12 Hz. For power correlations, the wavelet transforms of the LFP signals in each structure were computed and theta power over time was obtained by averaging the absolute values of the wavelet transforms in the 4-12 Hz range. For some analyses we also computed the partial theta power correlation between two regions that took into account theta power in a third area using the MATLAB function partialcorr.

Pharmacological inactivation of the ventral hippocampus

A 26-gauge guide cannula (Plastics One, Roanoke, VA, USA) was implanted in the vHPC using the surgical procedures described above. A single tungsten wire was glued to the side of the cannula so that it extended 1.5mm past the cannula tip. Tungsten wires were also bilaterally implanted in the mPFC and dHPC. After recovery from surgery, mice were food deprived to 85% of their pre-operative weight. Saline or muscimol (Tocris Bioscience, Bristol, UK) dissolved in saline (8.8 mM concentration) was microinfused into the vHPC by back loading into a 33 gauge infusion cannula and into polyethylene (PE 20) tubing connected to 1.0 ul Hamilton microsyringe (Hamilton Company, Reno, NV, USA). The infusion cannula protruded 1mm beyond the guide cannula tip. An infusion volume of 0.13 ul was delivered using a Harvard 11 Plus syringe pump (Harvard Apparatus, Holliston, MA, USA) at a rate of 0.13 ul/min. The time course of the experiment was as follows. First, saline was injected while the animal was in the homecage. This was followed by a 20-30 minutes post infusion interval, after which neural activity was recorded for 10 minutes while animals navigated the T-maze. Next, animals received either a second infusion of saline or muscimol, again followed by a 20-30 minute post infusion interval and a 10-minute recording as animals navigated the T-maze. Data analysis was restricted to periods when animals were moving at a consistent speed (5-9 cm/s). Coherence and power were calculated with methods described above and compared with Wilcoxon sign-rank test.

Statistics

To compare mean theta power and peak frequency between each region in Figure 2.1 and to assess changes in mean sample-choice power, coherence, power correlation or partial correlation, and dHPC-mPFC coherence differences after muscimol in Figures 2.1-2.5, we utilized the Wilcoxon signed-rank test, a non-parametric test for related samples that cannot be assumed to be normally distributed. Using the MATLAB function signrank, we tested the null hypothesis that the difference between two related groups (ex. dHPC power in sample vs choice phase) comes from a distribution of zero median at 5% significance level. In Figure 2.2, 2.3 and 2,6 correlation between two groups was tested with Pearson's test where r is the correlation coefficient between -1 (total negative correlation) and 1 (total positive correlation) with an r of 0 being no correlation.

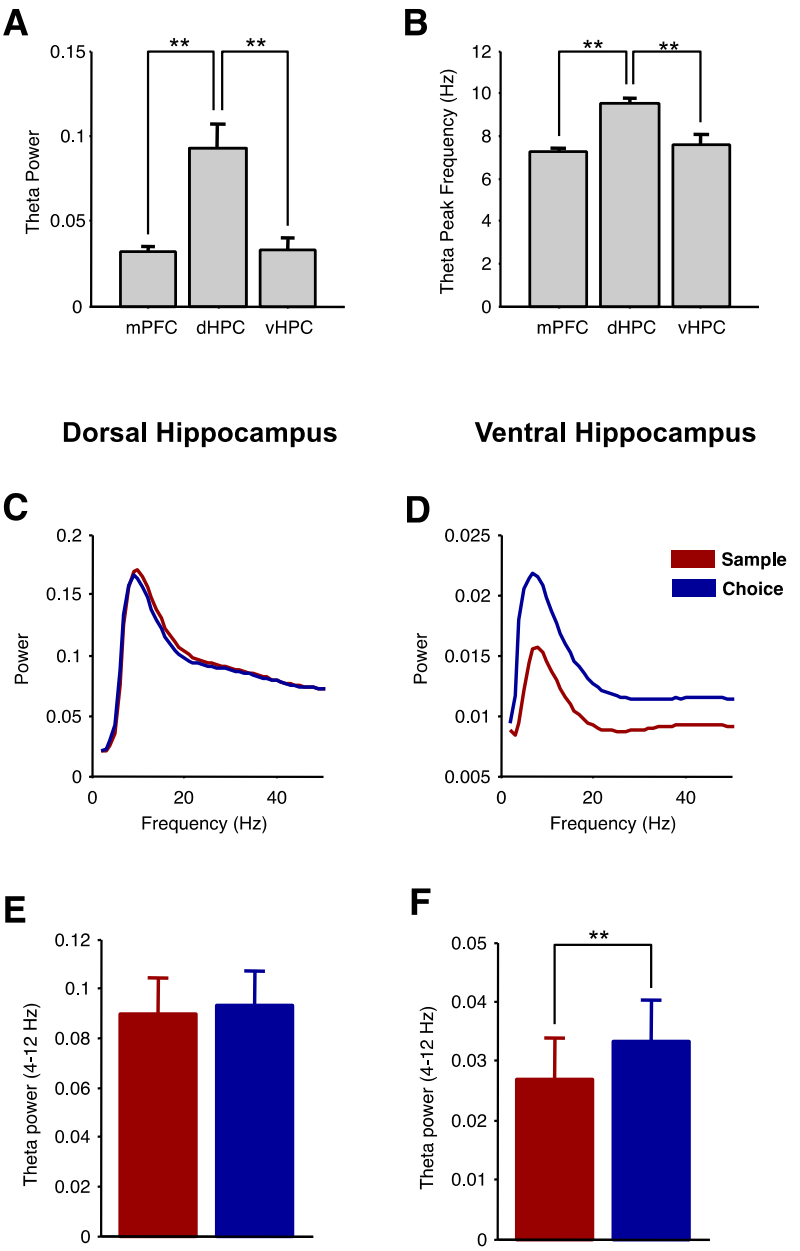

Figure 2.1. Modulation of hippocampal theta oscillations by spatial working memory. **A**, **B,** Power (**A**) and frequency (**B**) of theta oscillations recorded in the mPFC, dHPC and vHPC. Note the similarity of mPFC and vHPC theta oscillations. **C**, **D,** Example power spectra of LFPs recorded in the dorsal (**C**) and ventral (**D**) hippocampus of one animal during sample and choice phases. **E, F,** Theta power in dorsal (**E**) and ventral (**F**) hippocampus during sample and choice phases. Note that theta power increases in the choice phase only in the ventral hippocampus. Error bars represent mean ± s.e.m across animals (n=5-10); **P<0.01.

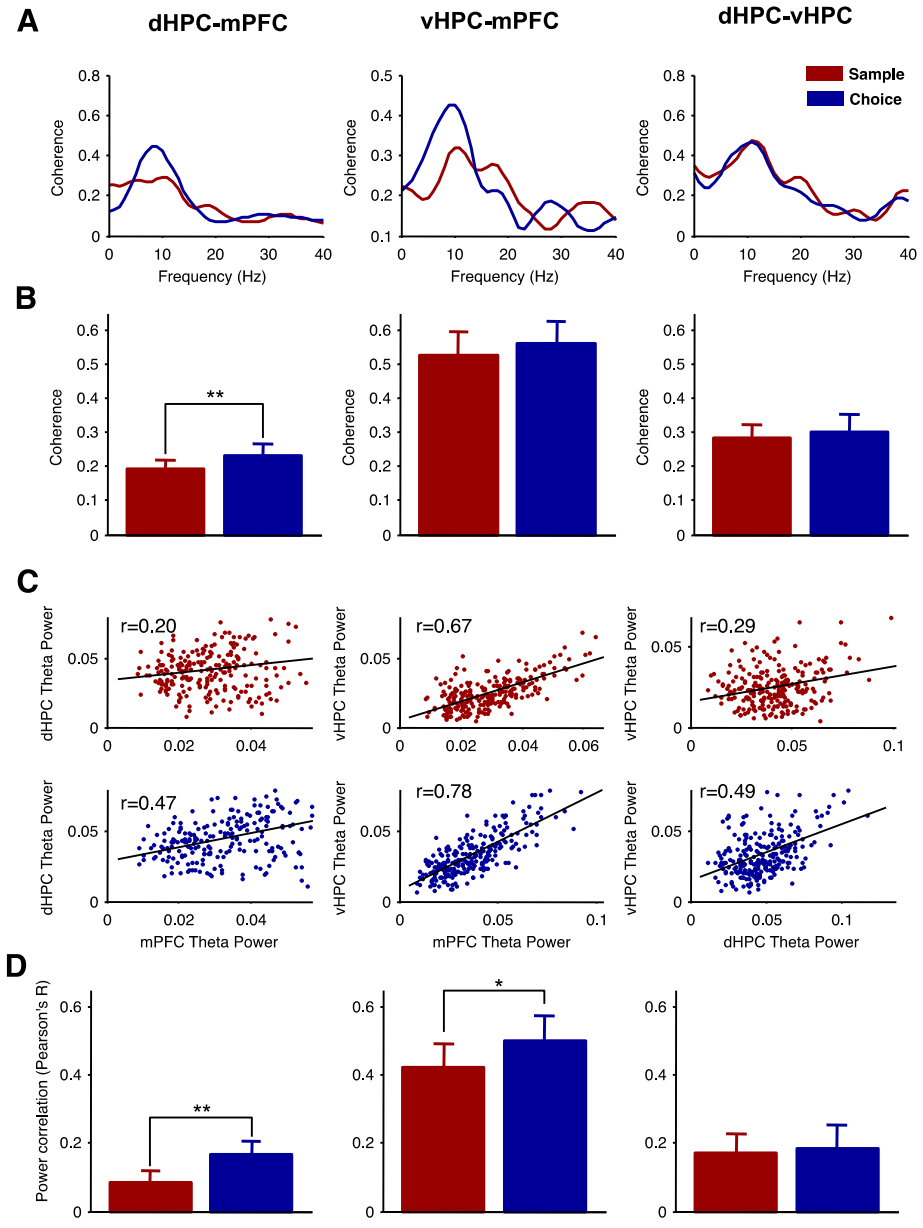

Figure 2.2 Hippocampal-prefrontal theta synchrony is modulated by the spatial working memory task. The columns illustrates synchrony between dHPC and mPFC (left), vHPC and mPFC (middle) and dHPC and vHPC (right). **A,** Examples of coherence during sample and choice phases in individual animals. **B,** Mean theta coherence during sample and choice phases. **C,** Examples of theta power correlations during sample and choice phases in individual animals. **D,** Mean theta power correlations during sample and choice phases. Note that theta synchrony increases between both hippocampal sub regions and the mPFC whereas intra-hippocampal synchrony remains unchanged. Error bars represent mean ± s.e.m across animals. *P<0.05; **P<0.01.

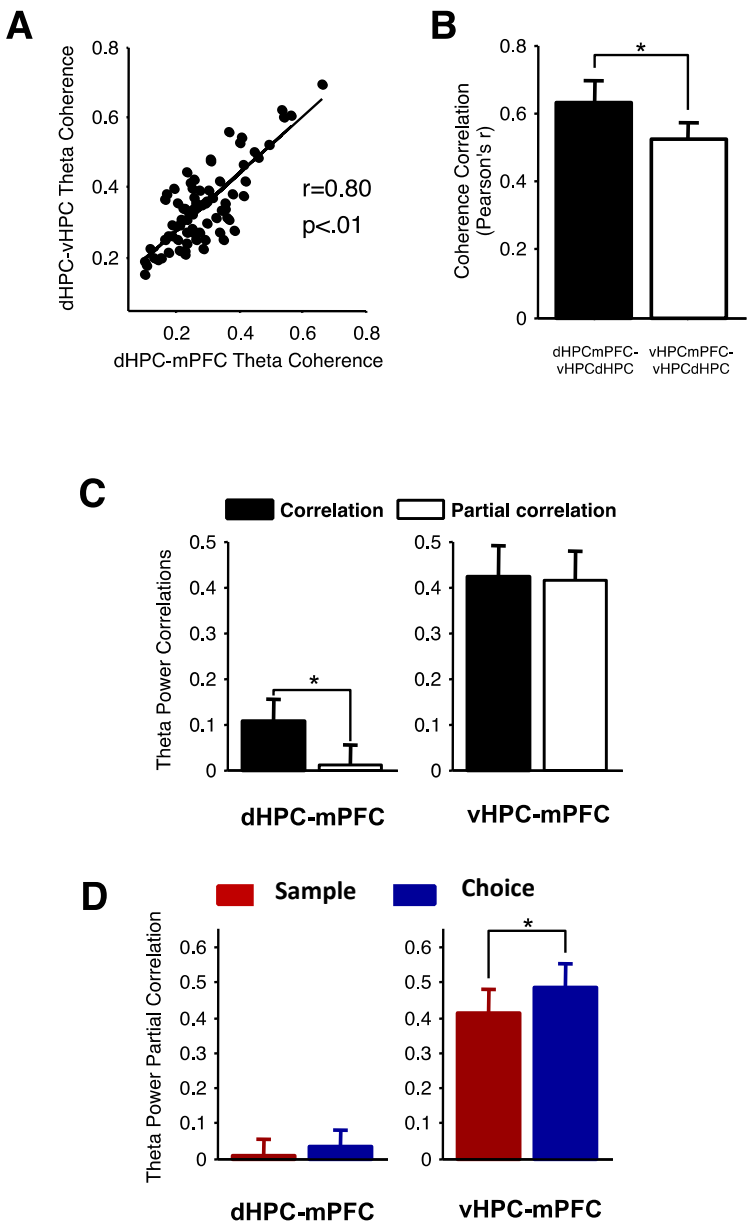

Figure 2.3 Hippocampal-prefrontal synchrony is correlated with ventral hippocampal activity. A, Positive correlation between dHPC-mPFC and dHPC-vHPC coherence in an example animal. **B,** Mean correlations between dHPC-mPFC and dHPC-vHPC theta coherence **C,** Mean theta power partial correlations. Note that partial correlations are lower for dHPC-mPFC but not vHPC-mPFC. **D.** Partial correlations during sample and choice phases. While an increase in vHPC-mPFC sample-choice power correlation is unaffected after removing the influence of dHPC (right), dHPC-mPFC correlation is no longer significantly different between sample and choice after removal of vHPC influence (left). Error bars represent mean ± s.e.m across animals (n=11); *P<0.05; **P<0.01.

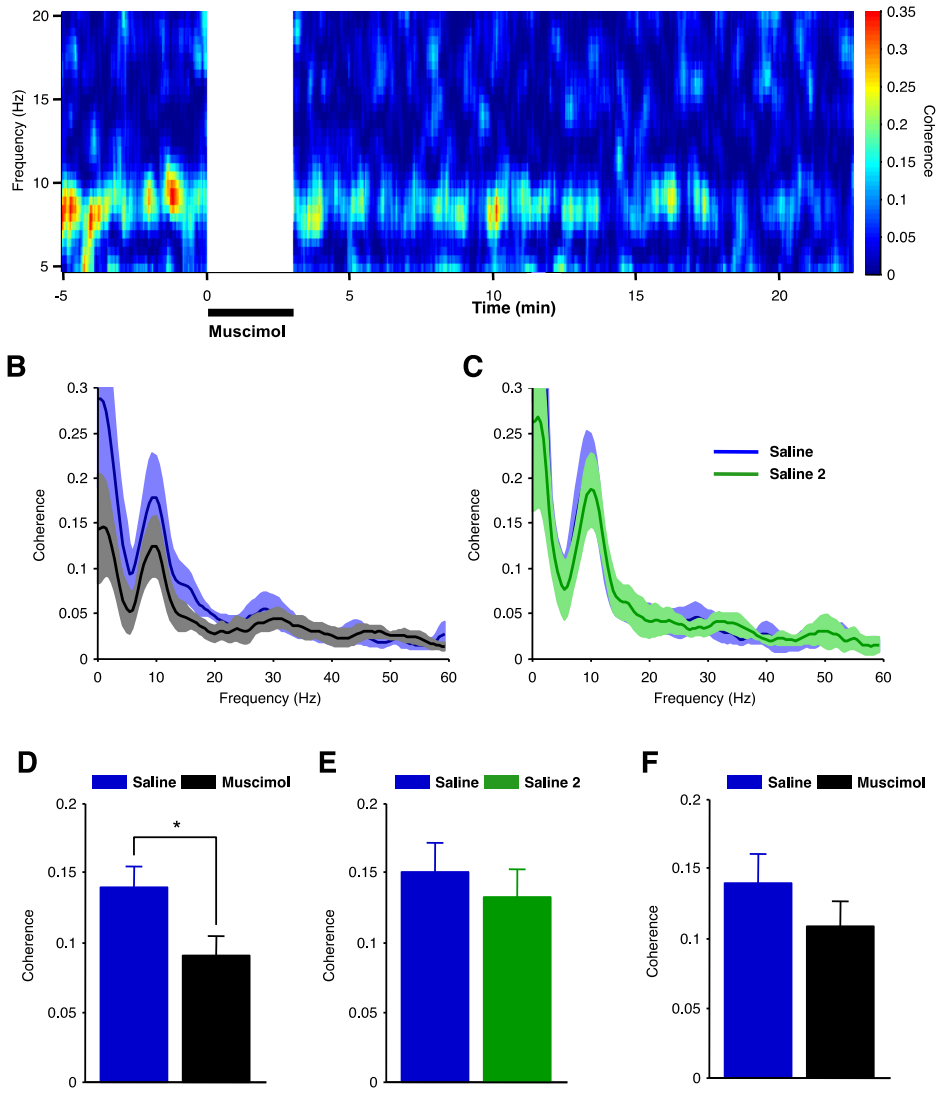

Figure 2.4 The ventral hippocampus is required for hippocampal-prefrontal theta synchrony. A, dHPC- mPFC coherence over time before and after muscimol infusion in one animal. **B,** Mean dHPC-mPFC coherence following muscimol or saline infusions. Note the decrease in theta coherence compared to saline infusion. **C,** Mean coherence following a second infusion of saline. **D**, Mean coherence between the dHPC and mPFC following infusions of saline and then an injection of muscimol into the ipsilateral vHPC. **E,** Mean coherence between the dHPC and mPFC following infusions of saline and then a second saline infusion (saline 2) into the ipsilateral vHPC. **F,** Mean coherence between the dHPC and mPFC following infusions of saline and then muscimol into the contralateral vHPC. Note the selective reduction of theta coherence following inactivation of the vHPC ipsilateral to the recording sites. Error bars represent mean ± s.e.m across animals (n=10); *p=0.01.

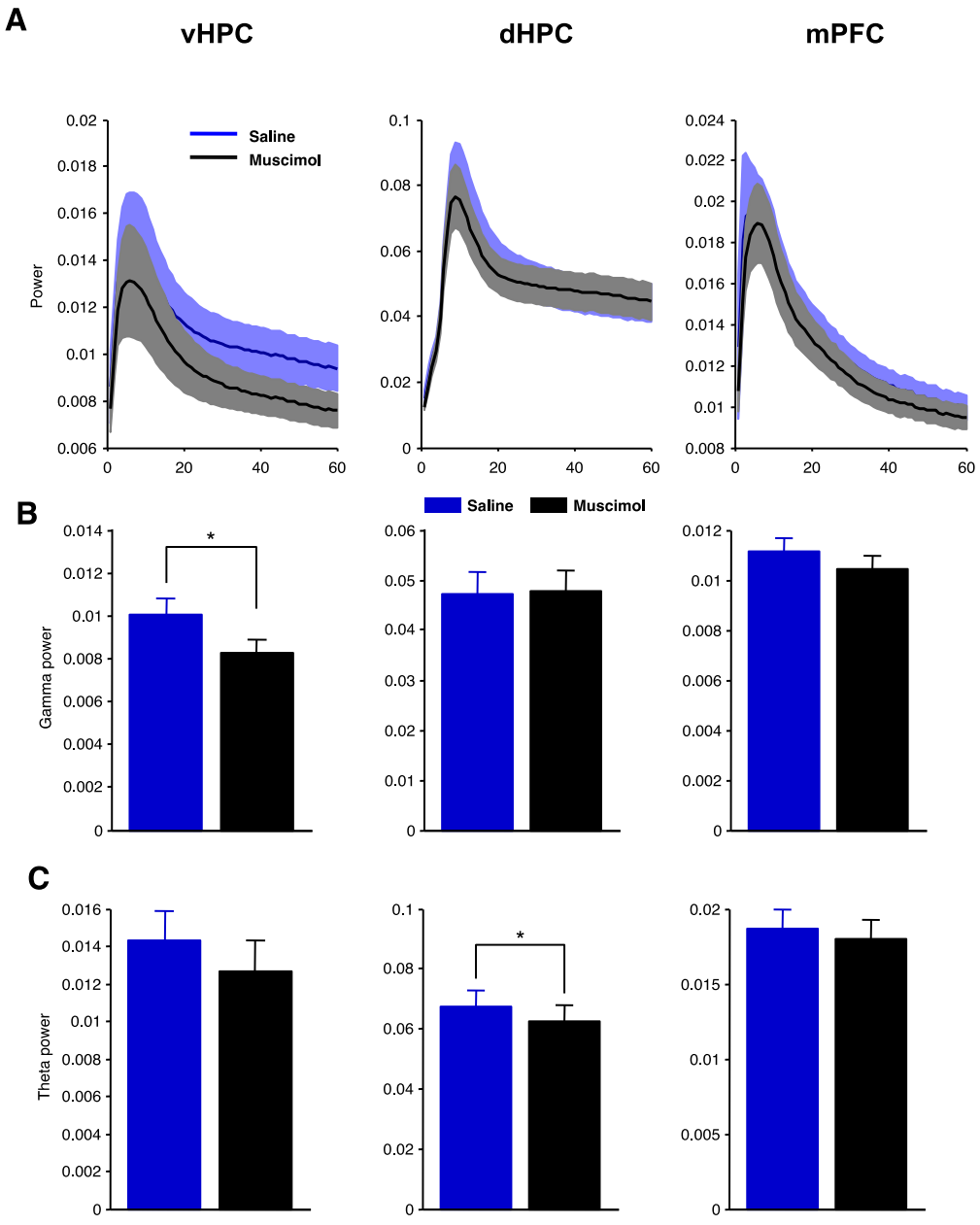

Figure 2.5 Effect of vHPC inactivation on theta and gamma oscillations in the hippocampus and prefrontal cortex. A, Power spectra of vHPC, dHPC and mPFC following saline and muscimol infusions into the vHPC. B, C, Mean gamma (B) and theta (C) power in vHPC, dHPC and mPFC following saline and muscimol infusions into the vHPC. Error bars represent mean ± s.e.m across animals (n=12 mice); *p<0.01.

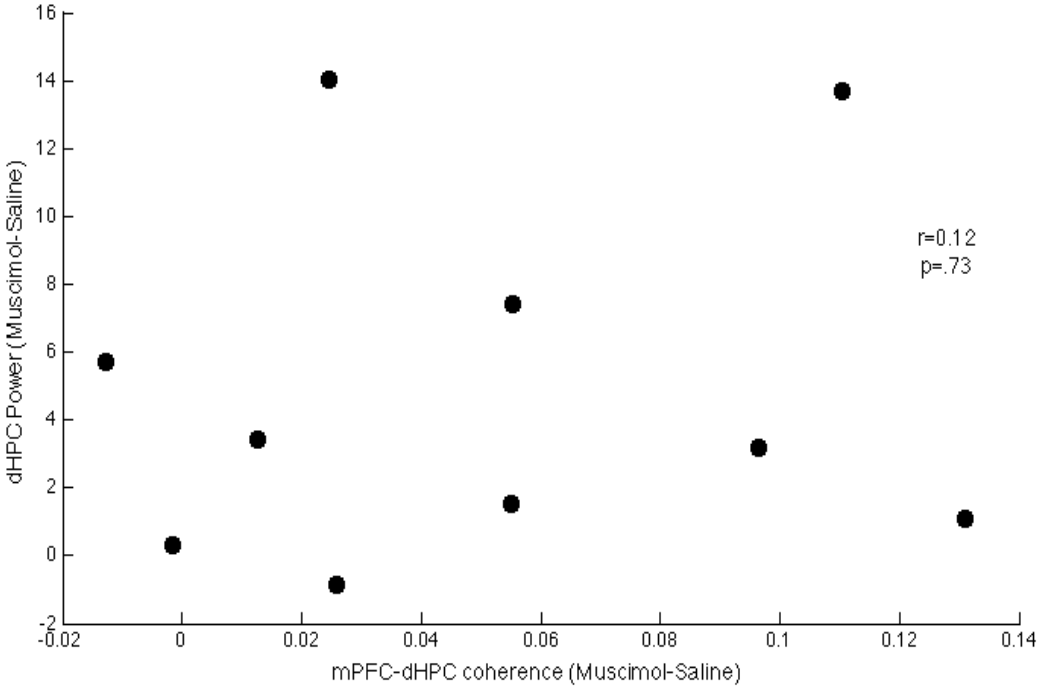

Figure 2.6 dHPC-mPFC coherence after muscimol is not correlated with dHPC power decrease. Change in dHPC power for each animal (n=10) does not correlated with change in dHPC-mPFC coherence (r=0.12, p>>.05)

Chapter 3

Inhibition of medio-dorsal thalamus disrupts thalamo-frontal connectivity and cognition

CHAPTER 3: INHIBITION OF MEDIODORSAL THALAMUS DISRUPTS THALAMOFRONTAL CONNECTIVITY AND COGNITION

(Note: These experiments were completed in collaboration of Sebastien Parnaudeau, Ph.D., a post-doctoral fellow in the lab of Christoph Kellendonk, Ph.D. in the Pharmocology Department at Columbia University.)

3.1 Introduction

As reviewed in chapter 1, studies on schizophrenia patients consistently identify altered activity in the PFC, which led to the prevailing hypothesis that the cognitive symptoms of schizophrenia, including working memory deficits, are due to prefrontal dysfunction (Weinberger and Berman, 1996). But several studies have also noted abnormal activity in other brain structures including the medial dorsal thalamus (MD), which has dense excitatory projections into the PFC (Jones 2007). Interestingly, several groups have reported altered correlation of activity between the MD and PFC at rest and during tests of cognition. (Minzenberg et al, 2009; Mitelman et al, 2005). These findings suggest that altered MD activity and/or impaired communication between the MD and PFC could play a role in the cognitive deficits seen in schizophrenia patients.

A major limitation of brain imaging studies is that they cannot draw causal relationships between measured physiological alterations and specific symptoms. As such, it remains unclear whether decreased MD activity is a cause or a consequence of schizophrenia and its associated cognitive dysfunction. Lesion studies in animal models have made a first step toward a better

understanding of the roles of the PFC and the MD in executive function. While such studies clearly involved the PFC in executive function in humans (Bechara et al. 1998; Hornak et al. 2004)nonhuman primates (Funahashi et al. 1993; Rygula et al. 2010) and rodents (Schoenbaum et al. 2002; Kellendonk et al. 2006), the function of the MD in cognition is more controversial. Whereas a number of groups have reported an impairment in working memory and reversal learning tasks in MD lesioned rats (Bailey and Mair, 2005; Floresco et al., 1999; Hunt and Aggleton, 1998), several other studies did not observe such effects (Beracochea et al., 1989; Hunt and Aggleton, 1991; Neave et al., 1993).

The interpretation of lesion studies is difficult in the context of imaging studies. Indeed, imaging studies have merely reported a decrease in the activity of the MD, while lesion studies physically and irreversibly ablate the entire structure. Imaging studies further suggest that the MD cooperates with the PFC during cognitive processes, but the nature of this relationship cannot be addressed by lesion studies in which both structures do not remain intact. To address these questions and to circumvent these limitations, we therefore used a recently developed pharmacogenetic approach, the DREADD (designer receptor exclusively activated by a designer drug) system (Armbruster et al. 2007; Ray et al. 2011; Garner et al. 2012) to selectively and reversibly decrease neuronal activity in the MD of mice performing a spatial working memory task. We found that a relatively mild decrease in the activity of MD neurons is sufficient to trigger selective impairments in a delayed nonmatching to sample (DNMS) working memory task. To investigate the nature and the role of MD-PFC communication in working memory, we recorded simultaneously from both structures in mice performing the DNMS task. We found that synchronous activity between MD and medial PFC (mPFC) increased hand in hand with

choice accuracy during the learning of the task and that reducing MD activity delayed both learning and the strengthening of synchrony. Interestingly, in trained animals, the strength of MD neurons phase-locking to medial prefrontal oscillations in the beta frequency range (13–30 Hz) increased specifically during the choice phase of the task associated with peak mnemonic demand, suggesting a role for MD-PFC beta synchrony in working memory. Strikingly, a primary decrease in the firing of MD neurons selectively disrupted this task-specific increase in MD-PFC beta-synchrony. In conclusion, our results demonstrate a causal relationship between decreased MD activity and deficits in executive function. They further suggest thalamofrontal beta synchrony as a potential mechanism contributing to working memory.

3.2 Results

Decrease of Mediodorsal Thalamus Neuron Activity using the DREADD System

A modified human muscarinic receptor, hM4D, was coexpressed along with humanized renilla green fluorescent protein (hrGFP) selectively in the MD using an adeno-associated virus expression system (AAV2-hM4D-IRES-hrGFP) (Figure 3.1A). The hM4D receptor is activated solely by a pharmacologically inert compound, clozapine-*N*-oxide (CNO), and not by endogenous acetylcholine or any other neurotransmitter (Armbruster et al. 2007). Upon CNO activation, hM4D hyperpolarizes neurons through a G protein mediated activation of inward-rectifying potassium channels (Armbruster et al. 2007). Stereotactic injection of AAV2-hM4D-

IRES-hrGFP virus into the MD induced coexpression of both GFP (green) and hM4D as assessed by anti-HA immunostaining (red) (Figure 3.1B). At higher magnification, we observed that the hM4D is localized in the plasma membrane as well as in neuronal processes (Figures 3.1B and 3.1D). Co-staining with anti-NeuN antibodies revealed that GFP expression was exclusively neuronal (Figure 3.1C, top panel). Due to the absence of interneurons in rodent MD (Kuroda et al. 1998), all infected neurons should be relay projection neurons. Using AAV2.2, an average of 27% ± 6% of the MD neurons expressed the GFP with a peak at 66% ± 9.6% at the site of injection (Figure 3.1C, bottom panel). The virus spread almost entirely among the anterioposterior axis of the MD whereas it stayed constrained within the dorsoventral and lateromedial axis of the MD (Figure 3.1C and see Figure 3.2A). Consistent with the known anatomy of the MD (Kuroda et al. 1998), infected neurons projected to layers I and III/V of prelimbic and orbitofrontal cortices (Figure 3.1D).

To determine whether activation of hM4D would hyperpolarize thalamic neurons as has been shown for hippocampal neurons (Armbruster et al. 2007), we performed whole-cell patch-clamp recordings from thalamic slices. Fluorescently-identified neurons expressing hM4D were significantly hyperpolarized after CNO bath application, while the resting membrane potential of cells infected with a control virus expressing only hrGFP were not (Figure 3.3). To determine whether activation of hM4D reduces the activity of MD neurons in vivo, we performed multiple single-unit recordings from the MD of freely moving mice injected with AAV2-hM4D-IRES-hrGFP (MD_{hM4D} mice). For this experiment, mice were exploring a familiar environment, specifically a T-maze to which they had been previously habituated. Sixty-three single units were recorded

both after systemic injection of saline and 2 mg/kg CNO. The dose of CNO was chosen based on a previous study reporting high in vivo efficacy at doses between 1 and 5 mg/kg on locomotor activity and stereotypy in a transgenic mouse expressing the hM3Dq receptor within the forebrain (Alexander et al. 2009). CNO reduced the firing rate of a substantial portion of the MD units (Figures 3.4A-C). To quantify this effect, we first calculated the ratio of firing rates after saline and CNO for each unit; the distribution of ratios in the sample was significantly different than that expected by chance ($p < 0.01$, Wilcoxon signed-rank test) (Figure3.4B). We next compared firing rates after saline and CNO injections for each neuron independently. CNO decreased firing rate significantly ($p < 0.05$ by paired t test) in 30 neurons (48%). In an additional 11 units (17%), CNO increased the firing rate. Using a more stringent Bonferroni correction ($p < 0.0008$) 16 (25%) and 6 (9.5%) units were inhibited or activated by CNO, respectively. For both analyses neurons with decreased firing rate were overrepresented as a consequence of CNO treatment (Binomial test: $p < 0.01$, $p < 0.05$ for Bonferroni-corrected values). Importantly, CNO treatment did not completely silence MD neurons; the neurons with decreased firing rate showed an average decrease of 38.7% ± 5.3%. This decrease in firing rate was not related to changes in locomotor activity or to differences in the isolation of single units (Figures 3.5A–C). The CNO-mediated decrease in firing rate was not observed in wild-type mice that do not express hM4D, demonstrating its dependence on hM4D (Figure3.4B, inset). While hyperpolarization of thalamic cells can induce a shift in the firing pattern from a tonic to a bursting mode due to the activation of T-type Ca^{2+}channels (Jahnsen and Llinas 1984), we did not observe a significant change in the fraction of burst firing in vivo after CNO injection (Figure 3.5D).

Decreased MD activity and deficit in working memory performance

To address working memory, we performed a delayed non-matched to sample (DNMS) T maze task commonly used in rodents (Figure 3.6A). Deficits in both acquisition and performance of this task have been observed after lesioning or silencing the mPFC in rats and mice (Dias and Aggleton 2000; Kellendonk et al. 2006; Yoon et al. 2008). Similarly, decreasing MD activity with CNO led to a deficit in the acquisition of the task, as CNO-treated MD_{hM4D} mice took longer to reach learning criterion than controls (ANOVA followed by Newman-Keuls correction for group comparisons, $^{*}p < 0.05$) (Figure 3.6B). To determine whether decreasing MD activity also affects working memory performance, a second cohort of hM4D- and GFP-expressing mice was trained without CNO until they reached criterion. Working memory performance was then tested after CNO or saline treatment at delays ranging from 6 to 120 s. In this cohort the number of animals was underpowered for a statistical comparison of all four groups. Since the three control groups did not differ in their performance (data not shown), they were combined for their comparison with CNO-treated MD_{hM4D} mice. CNO-treated MD_{hM4D} mice performed as well as the controls on the shorter delays (6 and 30 s) but showed significantly poorer performance on longer delays (repeated ANOVA group effect, $^{**}p < 0.01$) (Figure 3.6C). The observed deficits were not due to a general attention deficit or deficits in learning the spatial contingencies of the task, as mice with decreased MD activity showed performance comparable to that of control mice in a T maze based spatial reference memory task (Figure 3.6D). Moreover, we did not observe any general alterations of locomotor activity or anxiety-like behavior as assessed in

open field and elevated plus maze tests that may interfere with performance in the DNMS T-maze task (data not shown).

Working Memory-Induced Modulation of Thalamo-prefrontal Beta Synchrony Is Disrupted by Low MD Activity

Based on imaging studies reporting deficits in functional connectivity between different areas of the brain in patients, the disconnection theory (Pettersson-Yeo et al. 2011) posits schizophrenia as a subtle but pernicious syndrome of decreased long-range connectivity. In agreement with this theory, alterations in functional connectivity between MD and PFC have been observed in patients engaged in executive function tasks, including working memory (Mitelman et al. 2005; Minzenberg et al. 2009). To determine whether spatial working memory in mice involved MD-PFC synchrony, we recorded neural activity simultaneously in the MD and mPFC of mice performing the T maze DNMS task. If MD-PFC synchrony is involved in working memory, it should specifically be modulated during the choice phase of the DNMS T-Maze task, when the mnemonic requirement is high. For example, recent studies have shown that theta-frequency synchrony between the dorsal hippocampus (dHPC) and mPFC is modulated by the DNMS task (Jones and Wilson 2005; Sigurdsson et al. 2010). These studies found that phase-locking of PFC units to the theta-frequency component of the hippocampal local field potential (LFP) was enhanced during the choice phase of the DNMS task (which requires working memory) compared to the sample phase (which does not).

We therefore examined MD unit phase-locking to mPFC LFPs across multiple frequency ranges in trained animals performing the DNMS T-maze task. In saline treated mice, the phase-locking of MD units to beta frequency (13–30 Hz), but not theta (4–12 Hz) or gamma frequency (40–60 Hz) PFC oscillations, was strengthened in the choice phase (two-tailed paired t test, $^{**}p < 0.01$) (Figure 3.7A) suggesting that MD-PFC synchrony in the beta range is selectively modulated by working memory. Looking at individual units, about half of units (17/40; 42.5%) noticeably increased their phase-locking to mPFC beta oscillations during choice phase while phase-locking did not change or decreased in 18/40 (47.5%) and 4/40 (10%) units, respectively (Figure 3.8A). Strikingly, the increase in MD-PFC beta synchrony was selectively disrupted in CNO-treated MD_{hM4D} mice (repeated ANOVA, task phase × treatment interaction, $\#p < 0.05$) (Figure 3.7A). This was observed as well in mice that never received CNO injection prior the recording ruling out that these effects could be due to chronic effects of the drug (Figure 3.8E). Phase-locking to other frequency ranges was unaffected. Examining individual cells, we observed a significant reduction (Odd ratio = 0.09, $p < 0.001$) of the percentage of neurons increasing their phase-locking between sample and choice (2/33; 6.1%) and a significant increase (Odd ratio = 5.5, $p < 0.01$) of the percentage of cells showing no changes (27/33; 81.8%) in CNO-treated mice compared to controls (Figure 3.8A).

To rule out the possibility that CNO-treatment affected the quality of unit isolation, we confirmed that this disruption in MD-PFC beta synchronization was not due to differences in unit quality (Figures 3.8B and C). To examine the specificity of disrupted communication between the MD and mPFC we also measured synchrony between the MD and the dHPC, a structure that is also important for spatial working memory. While no task-related modulation

of phase-locking strength was observed in the beta and gamma range, a decrease of phase-locking between MD single-unit activity and dHPC theta-oscillations occurred during the choice phase of the DNMS task (Figure 3.7B; two tailed paired t test, $^{***}p < 0.001$). However, this decrease was not altered by CNO treatment (Figure 3.7B). Power spectra in the MD and mPFC were unchanged by CNO, suggesting that the effects of reducing MD activity were specific to the connectivity between the two regions rather than alterations in the strength of oscillations in either region (Figure 3.8D). We also examined the effects of CNO task-related firing in the recorded MD units, examining whether firing rates in the start arm of the T maze were modulated across sample versus choice, right versus left, or error versus correct trials. In saline treated mice, 40% (21/51) of our recorded units were firing in a task-related manner. We saw a nonsignificant trend toward a reduction in the percentage of task-related MD cells in CNO-treated mice as 31% (17/54) exhibited task-related activity.

Together, these results suggest that decreasing MD activity may impair working memory by disrupting MD-PFC beta synchrony during the choice phase of the task. In line with this interpretation, we found an increase of the proportion of MD cells significantly phase-locked to mPFC beta oscillations when trained control mice were performing the task (61/69 cells, 88%) compared to mice that were simply exploring the maze (15/59 cells, 25%) (Odds ratio = 22.37, $p < 0.001$). Lag analysis revealed a predominant MD to mPFC directionality in the beta-frequency range. Phase-locking of each MD unit was calculated repeatedly after systematically shifting the MD action potentials forward and backward in time relative to the mPFC LFP(Siapas et al. 2005). MD units tended to phase-lock strongest to the mPFC beta-frequency oscillation of

the future (mean lag, +20 ± 1.4 ms, Wilcoxon signed-rank test $p < 0.05$, $n = 76$) (Figure 3.9). This finding is consistent with the possibility that information tends to flow from the MD to the mPFC during the DNMS task.

Beta-Frequency Synchrony Parallels Behavior during Working Memory Task Acquisition

The parallel effects of MD inhibition on phase-locking and behavior after successful task acquisition suggest a role for the MD and MD-PFC connectivity in working memory performance. Yet CNO-treated MD_{hM4D} mice also had a deficit in task acquisition (Figure 3.6B). To determine whether altered MD-PFC functional connectivity could account for the deficits observed in task acquisition observed in CNO-treated MD_{hM4D}mice, we examined MD-PFC synchrony in an additional cohort of MD_{hM4D} mice treated with daily injections of CNO or saline during acquisition of the DNMS T-maze task. Because the training period is too brief to permit recording of a sufficient sample of MD units, coherence between MD and PFC LFPs was used to measure synchrony. As with the first cohort, CNO-injected MD_{hM4D} mice took significantly longer to acquire the task than saline-injected MD_{hM4D} mice. Consistent with a role for MD-PFC connectivity in task learning, LFP coherence between these two structures increased with task acquisition in both CNO- and saline injected MD_{hM4D} mice (Figure 3.10A). Strikingly, coherence in beta-frequency range increased hand in hand with performance (Figure 3.10B). In control mice, increases in coherence and choice accuracy occurred simultaneously at the end of the second session (trials 15–20). In contrast, both coherence and choice accuracy started to increase later in CNO-treated MD_{hM4D} mice (session 5, trials 41–45) (repeated ANOVA followed by Fischer correction, difference versus trials 1-5: $^{\circ}p < 0.1$, $^{*}p < 0.05$, $^{**}p < 0.01$, $^{***}p < 0.001$). In

addition, we did an analysis of correlation between coherence and performance for each session and each individual animal and found that coherence correlated significantly with behavioral performance for both saline- and CNO-treated MD_{hM4D} mice (Figure 3.10C). Finally, the parallel increase of coherence and performance was also seen in the theta-frequency range. In contrast, while gamma-frequency coherence also increased between early and late training phases in both saline and CNO-treated MD_{hM4D} mice, these increases did not correlate with increases in choice accuracy (data not shown). These data, together with the phase-locking findings, demonstrate that inhibition of MD disrupts both MD-PFC functional connectivity and working memory behavior in parallel, during task acquisition as well as task performance.

3.3 Discussion

Imaging studies have repeatedly reported deficits in MD and PFC activation in schizophrenia patients performing cognitive tasks. However, whether a decrease in MD activity can cause cognitive deficits is unclear. Moreover, the potential role for MD-PFC dysconnectivity in the generation of cognitive symptoms still remains unexplored. Here, by inducing a subtle decrease in the firing of MD neurons, we triggered selective deficits in a prefrontal-dependent task that addresses working memory impairments in patients with schizophrenia. We further found that beta range synchrony between the MD and the mPFC is modulated by working memory, and that this modulation is disrupted by the decrease in MD activity. Finally, during DNMS task acquisition, the magnitude of MD-PFC coherence increased in tight correlation with choice accuracy and both increases were delayed by inhibition of MD activity. Together these data demonstrate that decreased MD activity disrupts functional communication within the MD-PFC

circuit and causes deficits in prefrontal-dependent cognition. Our findings are consistent with a role for MD-PFC synchrony in working memory tasks and further support the possibility that thalamic deficits can causally contribute to cognitive dysfunction.

The Role of MD Activity in Working Memory

We showed that a decrease in MD activity induced a deficit in the acquisition in a DNMS working memory task. This impairment is not due to a deficit in general attention or deficits in learning the spatial contingencies of the task because CNO-treated MD_{hM4D} mice had no problems in learning a spatial version of the T maze task. Decreasing MD activity not only impaired the acquisition but also the performance of the DNMS task in trained animals, sparing performance at short (6 to 30 s) delays but impairing performance at long delays (60 to 120 s). One brain area that is implicated in working memory and receives direct projection from the MD is the mPFC. Deficits in both acquisition and performance of the DNMS T-maze task have been observed after lesioning or silencing the mPFC in rats and mice (Kellendonk et al., 2006; Yoon et al., 2008). We therefore hypothesize that disrupted communication between the MD and mPFC may underlie the observed deficit in the working memory task. Our electrophysiological findings discussed below are in line with this interpretation.

MD-PFC Functional Connectivity during Working Memory

Here, we report increases in synchrony between the MD and mPFC during a spatial working memory task in control mice. During task acquisition, synchronized activity between these two structures in the theta- and beta-frequency ranges increased hand in hand with improvements in task performance. After successful acquisition, beta-frequency synchrony was specifically

enhanced in the working memory-requiring choice phase of the task, during which mice need to keep information online to make the correct choice and obtain the reward. Finally, lag analysis demonstrated that the MD leads the mPFC. These results are consistent with the hypothesis that information flows from the MD to the mPFC in support of working memory, similar to previous findings suggesting that hippocampal-prefrontal interactions are also involved (Jones and Wilson, 2005; Sigurdsson et al., 2010). The precise nature of the information contributed by MD inputs to the mPFC is unclear. Studies of MD single unit activity during visual working memory in non-human primates have suggested the possibility that MD units encode motor planning information (Watanabe and Funahashi 2012)Considering the known inputs to the MD from the basal ganglia and extrapolating from these findings, it may be that the MD transmits motor information to the PFC about the choice to be made during spatial working memory.

Our findings point to synchrony between the MD and mPFC in the beta-frequency (13 to 30 Hz) range as of particular relevance to the DNMS task. While the oscillations in the theta and gamma bands have been classically linked to working memory, the functional role of beta-band oscillations is less understood. However, recent studies performed in human and nonhuman primates point to a role for beta-band oscillations in cognitive processes. Specifically, elevations of beta-band activity in visual and prefrontal cortical areas have been observed during the delay phase of working memory tasks (Tallon-Baudry et al. 2001; Tallon-Baudry et al. 2004; Deiber et al. 2007; Siegel et al. 2009). Interestingly, beta-band activity has also been linked to motor activity. Indeed, numerous studies provide evidence that beta activity is decreased during voluntary movements and increased during holding periods following movement in a variety of

structures belonging to the motor system (for a review see Engel and Fries, 2010). Rather than reflecting a lack of movement, a recent hypothesis proposed that beta rhythm would be related to the active maintenance of the current sensorimotor set. According to this hypothesis, the role of beta oscillations in cognition would be of similar nature and may be enhanced if the status quo is given priority over distractive new signal, whereas gamma band activity may predominate if changes in stimulus are expected (Engel and Fries 2010). Therefore, beta oscillations may relate to top-down processing and the increase of MD-PFC beta coherence observed during the choice phase of the DNMS task may reflect the maintenance of the information previously acquired during the sample phase of the task.

MD-PFC Dysfunction in Schizophrenia

The current findings are of potential relevance to the understanding of cognitive deficits in schizophrenia. Imaging studies reported both deficits in MD and PFC (Andrews et al., 2006; Minzenberg et al., 2009; Weinberger and Berman, 1996) in patients with schizophrenia during cognitive tests. Moreover recent studies have found an altered correlation in the activity of MD and PFC, suggesting that impaired functional connectivity between these structures might underlie the cognitive difficulties (Minzenberg et al., 2009; Mitelman et al., 2005). Structural abnormalities in this circuit have also been reported (Byne et al. 2009). However, one limitation of brain imaging is the low temporal resolution that does not allow studying the complex spatial-temporal orchestration of brain activity that is thought to underlie cognition. EEG methods offer a better temporal resolution and some studies observed that synchronous activity of beta and gamma oscillations are decreased in the cortex of patients with schizophrenia (for a review see(Uhlhaas and Singer 2010)). Our results indicate that the

engagement of beta synchrony in working memory is not restricted only to cortical areas but could also extend to thalamocortical circuits, and more specifically, that beta-frequency oscillations may underlie thalamocortical communication during working memory performance.

Our results further suggest that disruption of MD-PFC beta synchrony could participate in the generation of cognitive deficits in schizophrenia. However, whether this disruption is of primary origin in schizophrenia is hard to determine due to the circular nature of the brain. Postmortem and structural brain imaging studies show morphological abnormalities in the MD that suggest a primary deficit of the MD, at least in a subpopulation of patients (Byne et al. 2009). However, the MD is also part of the well-described corticostriatal loops in which the striatum projects back to the cortex via the thalamus (Haber and Calzavara 2009). A primary role of the striatum for the pathogenesis of schizophrenia has been proposed (Simpson et al. 2010). An overexpression of striatal dopamine D2 receptors used as a model for increased D2 receptor function observed in patients has been shown to cause PFC-dependent cognitive deficits. These deficits included impairments in the here presented DNMS T-maze working memory task (Kellendonk et al., 2006). One possibility is therefore that altered striatal function could impact on the prefrontal cortex via altering MD activity. Measuring MD-PFC synchrony in striatal D2 overexpressing mice would be a useful test of this hypothesis.

The DREADD System as a Tool to Decrease MD Activity

In this study, we chose a pharmacogenetic approach to reversibly reduce MD activity. The DREADD system relies on a mutated human muscarinic G protein-coupled receptor that does

not respond to the endogenous ligand acetylcholine. The activation of these receptors can be achieved by intraperitoneal injection of a biologically inert synthetic compound, CNO. There has been concern regarding the potential retro-reduction of CNO to clozapine, a well-known atypical antipsychotic drug (Loffler et al. 2012). However, for several reasons, our results cannot be explained by this back metabolism. First, while CNO retro-reduction to clozapine has been observed in humans and guinea pigs (Jann et al. 1994) back metabolism could not be detected in rats and mice (Guettier et al. 2009). Second, CNO-treated GFP-expressing control mice did not show any alteration in any of the tested behaviors compared to saline groups. This includes behavior that has been shown to be sensitive to clozapine such as locomotor activity (McOmish et al. 2012). Finally, clozapine has been reported to alter MD firing (Lavin and Grace 1998). While we found a decrease in MD neuronal firing rate in MD_{hM4D} mice injected with CNO (Figures 3.4B,C) we did not see any firing rate changes in mice that do not express the hM4D receptor (Figure 3.4C, inset).

3.4 Methods

Animals

All protocols used in the present study were approved by the Institutional Animal Care and Use Committee (IACUC) at Columbia University. Mice were C57/Bl6 males purchased from Jackson Laboratory and housed under a 12 hr, light-dark cycle in a temperature-controlled environment with food and water available ad libitum. For the behavioral experiments, mice were food restricted and maintained at 85% of their initial weight. After testing, mice were sacrificed and

the expression as well as the location of GFP expression was verified to ensure that we correctly targeted the MD. Mice for which GFP was not visible or in an incorrect location were removed from the final analysis.

Drugs

Clozapine-N-Oxide (CNO) (Sigma) was dissolved in PBS to a final concentration of 0.2 mg/ml. PBS or CNO (2 mg/kg) was administered intraperitoneal to the mice 30 min before behavioral testing or in vivo recording (based on personal observations and Alexander et al, 2009). For thalamic slice physiology CNO was diluted into 1 µM with artificial cerebrospinal fluid. Fresh CNO solution was prepared on the day of usage.

Generation of AAV2-hM4D and Virus Injection

The AAV2-hM4D-IRES-hrGFP (called later AAV2-hM4D) virus was generated by inserting the hM4D sequence into the multiple cloning site of the pAAV-IRES-hrGFP vector (Agilent Technologies). The AAV2-hM4D-IRES-hrGFP and control (AAV2-hrGFP) viruses were produced by Vector Biolabs (Eagleville, PA). Mice were injected bilaterally with 0.5 µl of AAV2-hM4D (1.04×10^{13} particles/ml) or AAV2-hrGFP (1×10^{12}particles/ml). Viruses were pressure injected using a glass pipette (10–15 µm) into the MD (coordinates: A/P, −1.3 mm; M/L, ±0.35 mm; D/V, −3.2 mm). After each injection, the pipette remained in situ for 10 min to minimize leaking. Six-week-old mice were injected and then tested 4 weeks later for both behavioral and in vivo electrophysiology studies. For thalamic slice recordings, 3-week-old mice were injected and sacrificed 3 weeks later.

Histology and Immunostaining

Histology and immunostaining was performed using classical methods. HA rabbit-polyclonal (Invitrogen # 71-5500) antibody was diluted 1/1,000 in PBS and incubated overnight at 4 dC. Anti NeuN (Millipore, MAB377) HC was performed at a dilution of 1/100. The anti-rabbit Cy3 secondary antibody (Jackson laboratories) was diluted 1/1,000.

Nonmatching to Sample T Maze Task

We used the methods described previously (Sigurdsson et al, 2010). Animals were trained on a discrete non-match-to-sample spatial working memory task in a T- maze (dimensions 61 x 51 x 11cm). Mice were first habituated to the maze for two days during which they had 15 minutes to collect food pellets (20mg dustless sugar pellets, Bioserv). The next three days, mice were required to complete 4 forced runs each day in order to habituate to the guillotine doors. Mice were then tested on 10 trials per day, each trial consisting of two runs, a forced run and a choice run. At the beginning of the trial both arms are baited. In the forced run the right or left arm is randomly chosen to be open, while entrance to the other arm is blocked. To start the forced run, the mouse was placed at the long end of the T-maze. After running down the center arm of the maze, it was directed into the open goal arm where it had access to food.

Once the mouse reached back the starting arm, it was blocked for a brief delay (6 s) after which the choice run started. During the choice run, the mouse ran down the center arm, but now had to choose between two open goal arms. To obtain a reward, animals were required to enter the goal arm not visited during the sample phase. A correct choice was scored when the mouse visited in the choice run the alternate arm to the forced run. Animals were given daily

training sessions of 10 trials until they reached criterion performance, defined as performance of a minimum of seven trials correct per day for three consecutive days. The inter-trial time was 45 s. After the mice reached criterion, there performance was tested on different delays of 6 s, 30 s, 60 s, 90 s, 120 s and 180 s with 10 trials per delay.

Spatial T Maze Task

The spatial version of the T-maze used the same maze apparatus and habituation procedure than the nonmatching to sample task. Only the rule to acquire the task differed. For all trials each mouse was assigned one arm, left or right, as the baited target arm. Mice were trained ten trials per day and criterions were fixed at seven correct choices out of ten during three consecutive days.

Microdrive Construction and Surgery

Animals were implanted with multiwire microdrives using methods described previously (Adhikari et al, 2010). Custom microdrives were constructed using interface boards (EIB-32, Neuralynx, Bozeman, MT) fastened to machine screws (SHCX-080-6, Small Parts, Inc, Miramar, FL). Stereotrodes (14 per animal) were constructed of 25 µM Formvar-coated tungsten micro wire (California Fine Wire, Grover Beach, CA), fastened to a cannula attached to the interface board, and implanted in the MD. Single-wire, 75 µM tungsten electrodes were stereotactically placed into the medial PFC and cemented directly to the skull during surgery. Animals were anesthetized with isoflurane (0.5%–1.2%) in oxygen, and placed in a stereotactic apparatus (Kopf Instruments, Tujunga, CA) on a feedback-controlled heating pad. Anterior-posterior and medial-lateral coordinates were measured from bregma, while depth was calculated relative to

brain surface. Tungsten wire electrodes were implanted in the MD (−1.22, 0.30, and 2.7), in the medial PFC (+1.8, 0.4, and 1.65) and in dHPC. Animals were given analgesics (Carprofen, 5 mg/kg S.C.) and monitored postoperatively. After a suitable period of recovery, the MD stereotrodes were advanced until well-isolated single units were obtained.

Single unit isolation

When multiple units are recorded on the same electrode, waveform characteristics are used to separate out clusters of spikes that likely come from the same unit. We used a semi-automated process (Klustakwik, instantiated in SpikeSort3D from Neuralynx) to minimize subjective error. While no objective, firm cut-off criteria has been established, the accepted means of determining whether cluster quality affects results of single unit analysis is to correlate quantitative measures of cluster separation (such as Mahalobinis distance) with outcome variables (Schmitzer-Torbert et al. 2005)If, at low values of cluster separation values correlate with the variable of interest, standard practice dictates that one should remove clusters with these low values. Isolation distance can also be compared across groups. To determine whether our firing rate and phase locking results were affected by differences in quality of cluster isolation, for each cluster of spikes we computed the isolation (Mahalobinis) distance using four spike waveform features: the first two principal components, peak and energy using the built-in function in the SpikeSort3D software. There was no difference in cluster quality between treatment groups. In addition, we looked for and did not find any correlation between isolation distance and firing rate and phase locking, our principle outcome measures, either the entire sample or for the subsample with isolation distances less than 10. We therefore found no cause

to eliminate clusters with low isolation distances. Finally, to be doubly sure that our results were not compromised by units with low isolation distance, we repeated our analyses after eliminating all units with isolation distances less than 10. For the firing rate data, 49 of 63 original units (78%) were retained, of which 27 significantly decreased, 7 significantly increased and 15 showed no change, similar to the original result. For the phase locking data, 30 of the 33 units (91%) from the CNO group and 38 of the 40 units (95%) from the saline group were retained and we observed the same effects as in Figure 3.7A.

Behavior and Neurophysiological Data Acquisition

Mice used for "task-independent" MD single unit activity (Figure 3.4) were recorded during free exploration of the T maze. Mice were injected i.p. with saline solution and recorded 30 min after the injection during 15 min. After this, without moving the stereotrodes, mice were injected i.p. with CNO and recorded 30 min after the injection during 15 min. Mice used for "working memory task-dependent" recordings were performing the previously described T maze DNMS task during data acquisition. We restricted our analysis to neural activity in the center arm of the maze during sample and choice phases. This had the advantage of minimizing behavioral variability, as both trajectories and speeds of center-arm runs were comparable in saline- and CNO-treated and MD_{hM4D} mice. Recordings were obtained via a unitary gain head-stage preamplifier (HS-32; Neuralynx) attached to a fine wire cable. Field potential signals from MD, mPFC and dHPC sites were recorded against a screw implanted in the anterior portion of the skull. LFPs were amplified, band-pass filtered (1–1,000 Hz), and acquired at 1,893 Hz. Spikes

exceeding 40 μV were band-pass filtered (600–6,000 Hz) and recorded at 32 kHz. Both LFP and spike data were acquired with Lynx 8 programmable amplifiers on a personal computer running Cheetah data acquisition software (Neuralynx). The animal's position was obtained by overhead video tracking (30 Hz) of two light-emitting diodes affixed to the head stage.

Firing Rate and Burst Analysis

Data was imported into Matlab for analysis using custom-written software. Instantaneous firing rate for the example cell in was smoothed using Matlab smooth with a 60 s moving average. To test the significance of firing rate changes, we used both a population analysis and an individual cell analysis. For the population analysis we used a sign-rank test to determine whether the distribution of firing rate rations (CNO:SAL) were significantly different from a distribution with a median of 1. For the individual cell analysis each 15 min recording session under either saline or CNO conditions were separated into 30 s bins and firing rate was calculated. A one-factor ANOVA was performed on each cell to determine whether the mean firing rate after CNO was significantly different from that after SAL, with and without Bonferroni correction as described in the text. The predominance of decreases versus increases in firing rate using this method was then also tested using a Binomial test. For burst analysis, a burst was defined by the following criteria: maximum interval to start burst (i.e., the first interspike interval within a burst) must be = 4 ms; maximum interval to end burst, 10 ms; minimum interval between bursts, 100 ms; minimum duration of burst, 4 ms; and minimum number of spikes within a burst, two.

Phase-Locking Analysis

Phase-locking of MD units to mPFC LFPs was accomplished by fist filtering the field potentials in either the theta (4–12 Hz), beta (13–30 Hz), or gamma (40–60 Hz) range using a zero phase delay filter and computing phase using a Hilbert transform. Each unit spike was assigned a phase based on its simultaneous field potential sample. The magnitude of phase-locking was quantified mean resultant length (MRL) of the sum of the unit vectors representing the phases at which each spike occurred, divided by the number of spikes. The MRL is sensitive to the number of spikes used in the analysis. Therefore, to compare phase-locking strength by condition we computed the MRL for multiple (1,000) subsamples of 50 spikes per condition and averaged across subsamples for each condition, and for each unit. Units that fired fewer than 50 spikes in each condition were not analyzed. The statistical significance of phase-locking was assessed using the Rayleigh test for circular uniformity.

Directionality Analysis

Data were pooled for task independent and task dependent behavior sessions. Cells with fewer than 600 spikes during the entire recording session were not analyzed. To determine the temporal relationship between unit activity and beta oscillations in the mFPC, phase-locking was calculated for 50 different temporal offsets from the mPFC LFP for each unit recording. Only units with significant Bonferroni-corrected phase-locking in at least one of the 50 shifts are shown in Figure 3.8.

Field Potential Analysis

For coherence and behavior across learning, recordings were binned into early (first 5 trials), middle (trials 25–30), and late (last 5 trials on the day the animal achieved criterion

performance) trials. Coherence of the field potentials was computed using the multitaper method (MATLAB routines provided by K. Harris). Field potential samples for the trials in each bin were concatenated and then divided into 1,000 ms segments (800 ms overlap). The Fourier transform of each segment was computed after being multiplied by two orthogonal data tapers. Coherence was computed by averaging the cross-spectral densities of two field potential signals across data windows and tapers and normalizing to the power spectral densities of each signal. Beta coherence was computed as the mean coherence in the 13–30 Hz range.

Statistics

To test the significance of firing rate changes, we used both a population analysis and an individual cell analysis. For the population analysis we used a sign-rank test to determine whether the distribution of firing rate rations (CNO:SAL) were significantly different from a distribution with a median of 1 (Figure 3.4b). For the individual cell analysis each 15 min recording session under either saline or CNO conditions were separated into 30 s bins and firing rate was calculated. A one-factor ANOVA was performed on each cell to determine whether the mean firing rate after CNO was significantly different from that after SAL, with and without Bonferroni correction as described in the text. The predominance of decreases versus increases in firing rate using this method was then also tested using a Binomial test (Figure 3.4c).

To test differences between saline/cno groups in firing rate across speeds (Figure 3.5a) and the difference in spikes occurring in bursts, we used paired ttest with a 5% significance level. To determine if there was a significant difference between groups during acquisition and

performance of Tmaze we performed an ANOVA test followed by a Neuman Keuls post hoc analysis. To test for a significant difference in sample-choice phase locking for saline and cno group means we performed a repeated measures ANOVA.

The magnitude of phase-locking was quantified mean resultant length (MRL) of the sum of the unit vectors representing the phases at which each spike occurred, divided by the number of spikes. The MRL is sensitive to the number of spikes used in the analysis. Therefore, to compare phase-locking strength by condition we computed the MRL for multiple (1,000) subsamples of 50 spikes per condition and averaged across subsamples for each condition, and for each unit. Units that fired fewer than 50 spikes in each condition were not analyzed. The statistical significance of phase-locking was assessed using the Rayleigh test for circular uniformity.

In Figure 3.5c, 3.8b and 3.10c correlation between two groups was tested with Pearson's test where r is the correlation coefficient between -1 (total negative correlation) and 1 (total positive correlation) with an r of 0 being no correlation.

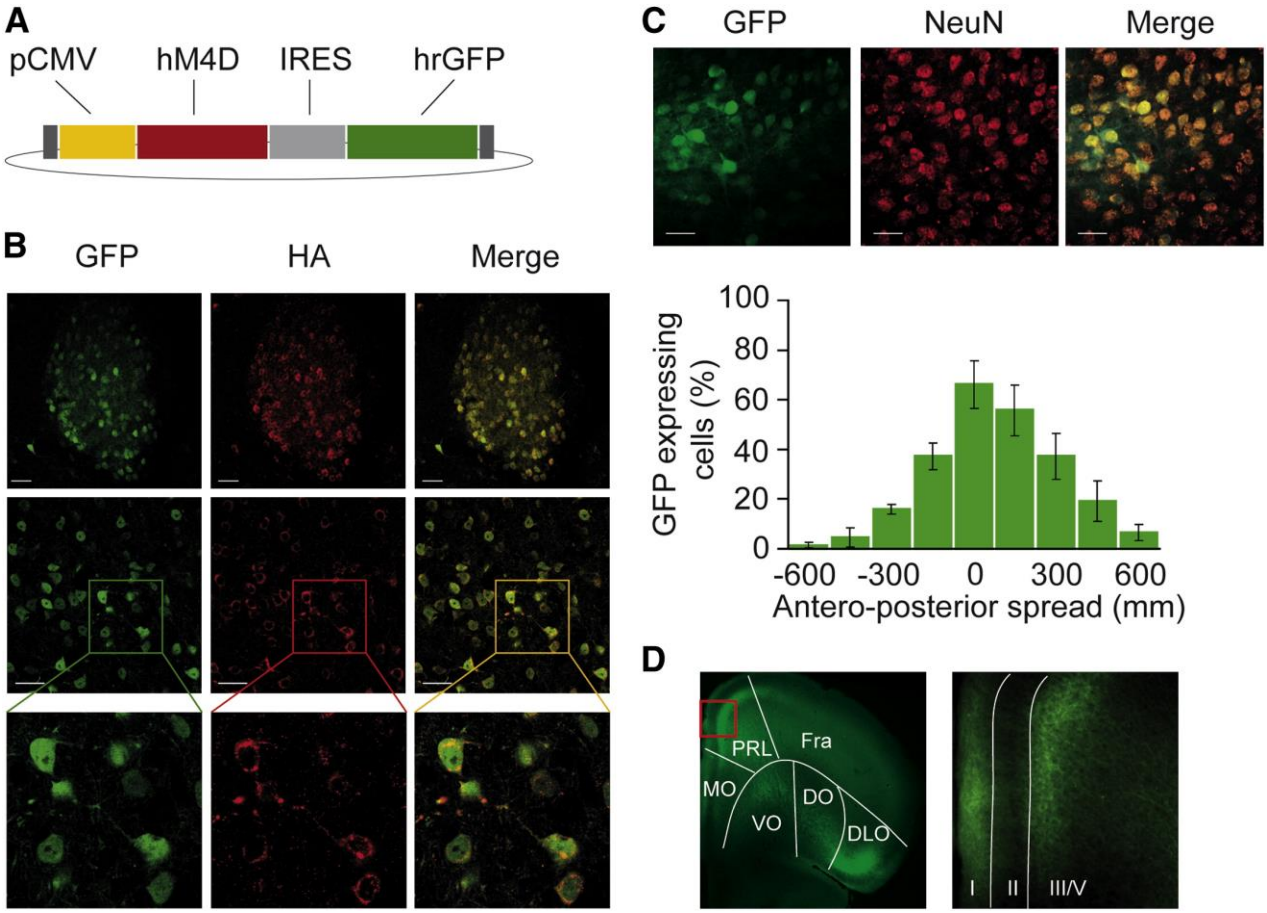

Figure 3.1 Expression of hM4D in the Mediodorsal Thalamus using a Viral Vector. A, Schematic drawing of pAAV2-hM4D-IRES-hrGFP plasmid. Both hM4D (red) and hrGFP (green) are expressed under the control of a cytomegalovirus (CMV) promoter (yellow). **B,** Native hrGFP fluorescence (green) and anti-HA immunostaining (red) reveal coexpression (yellow) of GFP and hM4D in MD cells. **C,**Top panel: native hrGFP and anti-NeuN immunostaining (red) reveal that hrGFP is exclusively expressed in neurons. Bottom panel: stereotactic injection of the AAV2-hM4D-IRES-hrGFP leads to transgene expression in 27 ± 6% of MD neurons with a peak at 66% ± 9.6% at the site of infection (n = 4). **D,** GFP labels the MD projections to the PFC after injection with a hrGFP control virus in the MD.Abbreviations: prelimbic (PrL), medial ventral orbital (VO), lateral orbital (LO) dorsolateral orbital (DLO), frontal associate (Fra) cortices, I, III/V depict cortical layers. Error bars: SEM.

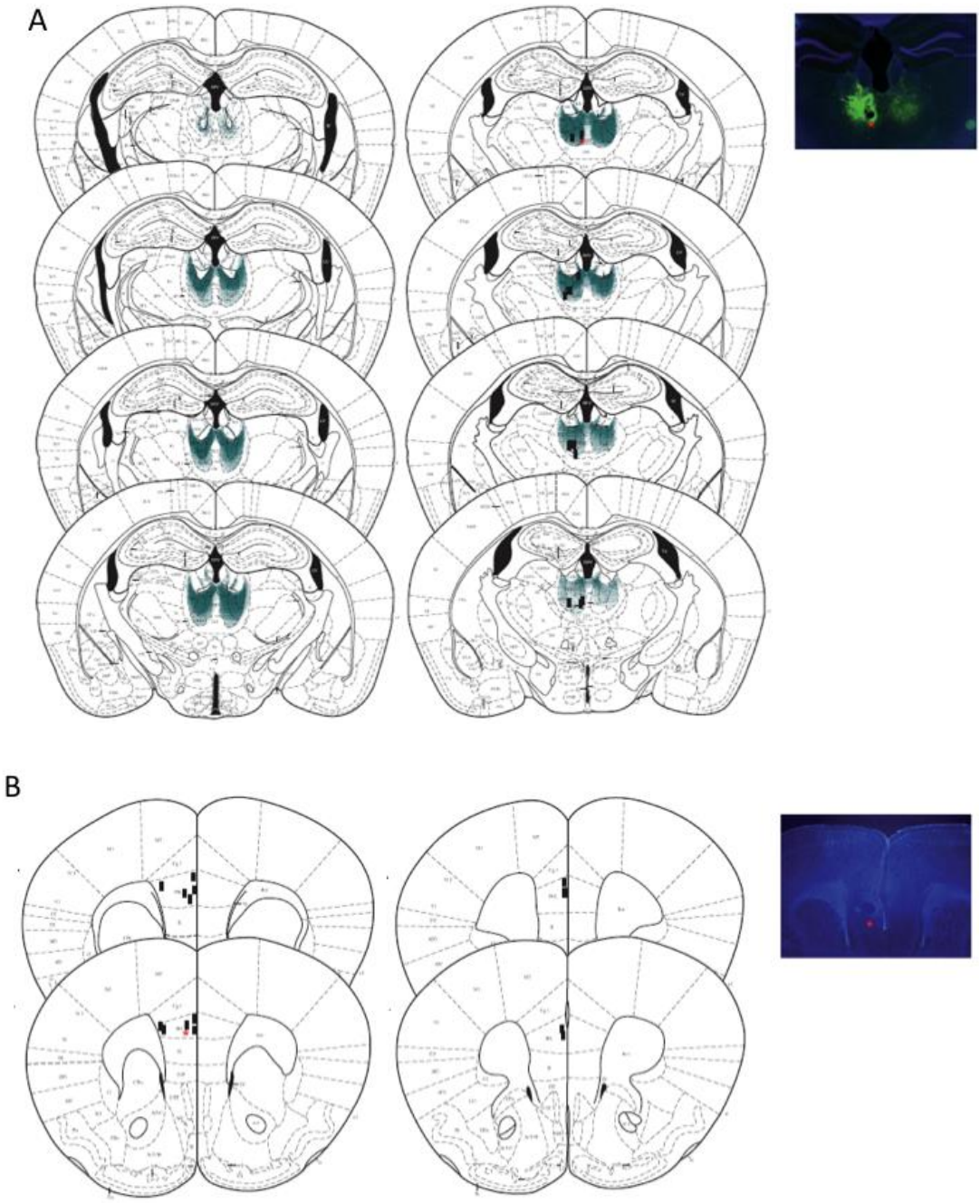

Figure 3.2 Extent of viral infection and electrode placement in the MD.
A,Representation of the viral spread in the MD for all the mice used in this study (blue). Electrode placements within the MD of the mice used for *in vivo* recordings are reported with black lines. Right: representative picture of a brain slice presenting hrGFP expression (green) within the MD and showing a lesion at the emplacement of the stereotrode (red star). **B,** Electrode placement within the medial PFC of the mice used for *in vivo* recordings. Right: representative picture of electrode placement as assayed by post-recording mPFC lesion, red star.

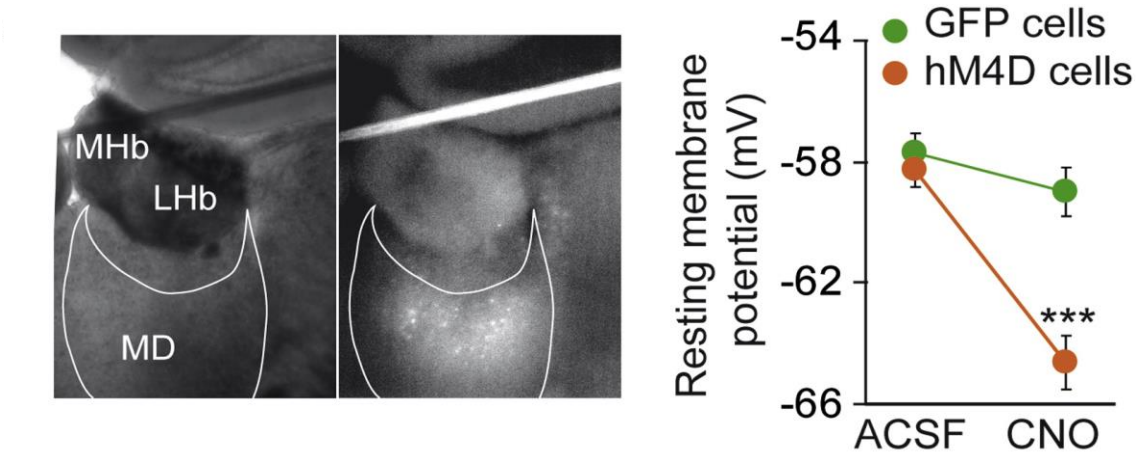

Figure 3.3 Decreasing Activity in the Mediodorsal Thalamus *in vitro* using a Pharmacogenetic Approach. Left panel: visualization of hM4D ires-hrGFP expressing neurons in a thalamic slice. Right panel: resting membrane potential of MD neurons infected with control hrGFP (green) and experimental hM4D ires hrGFP (orange) virus before and after bath application of 1 µM CNO (repeated-measures ANOVA, group × treatment interaction $^{***}p < 0.001$; n = 11 and 10 cells for hrGFP and hM4D-hrGFP cells).

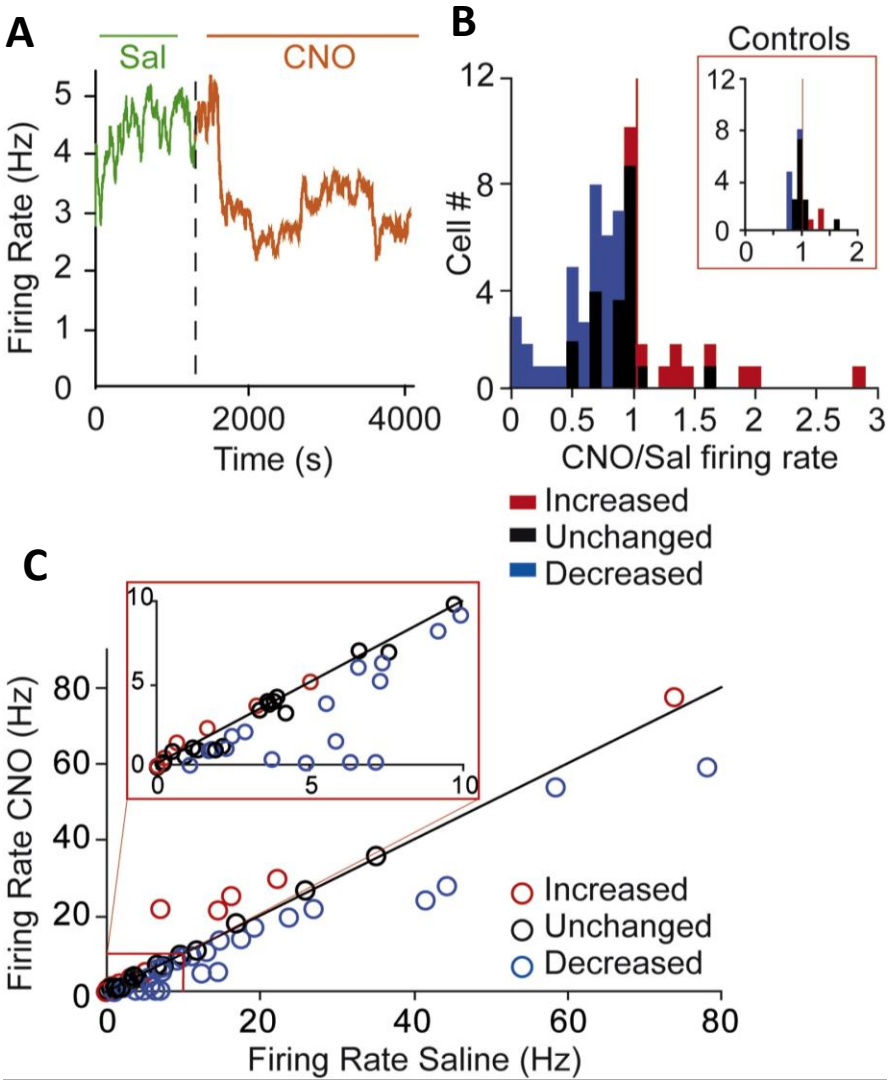

Figure 3.4 Decreasing Activity in the Mediodorsal Thalamus *in vivo* using a Pharmacogenetic Approach. A, Example of MD unit activity in vivo before (green) and after (orange) systemic injection of 2 mg/kg CNO to anMD_{hM4D} mouse. **B,** Histogram of the ratios of firing rate after CNO to firing rate after saline in MD_{hM4D} mice. Red and blue bars represent cells with statistically significant increases or decreases in firing rate, respectively. Inset: histogram of the ratios of firing rate after CNO to firing rate after saline in wild-type mice. **C,** Firing rate after saline versus firing rate after CNO for entire sample of 63 MD units. Red and blue circles indicate units with statistically significant increases or decreases in firing rate, respectively ($p < 0.05$, paired t test). Inset is a magnified view of lower firing-rate neurons.Error bars: SEM.

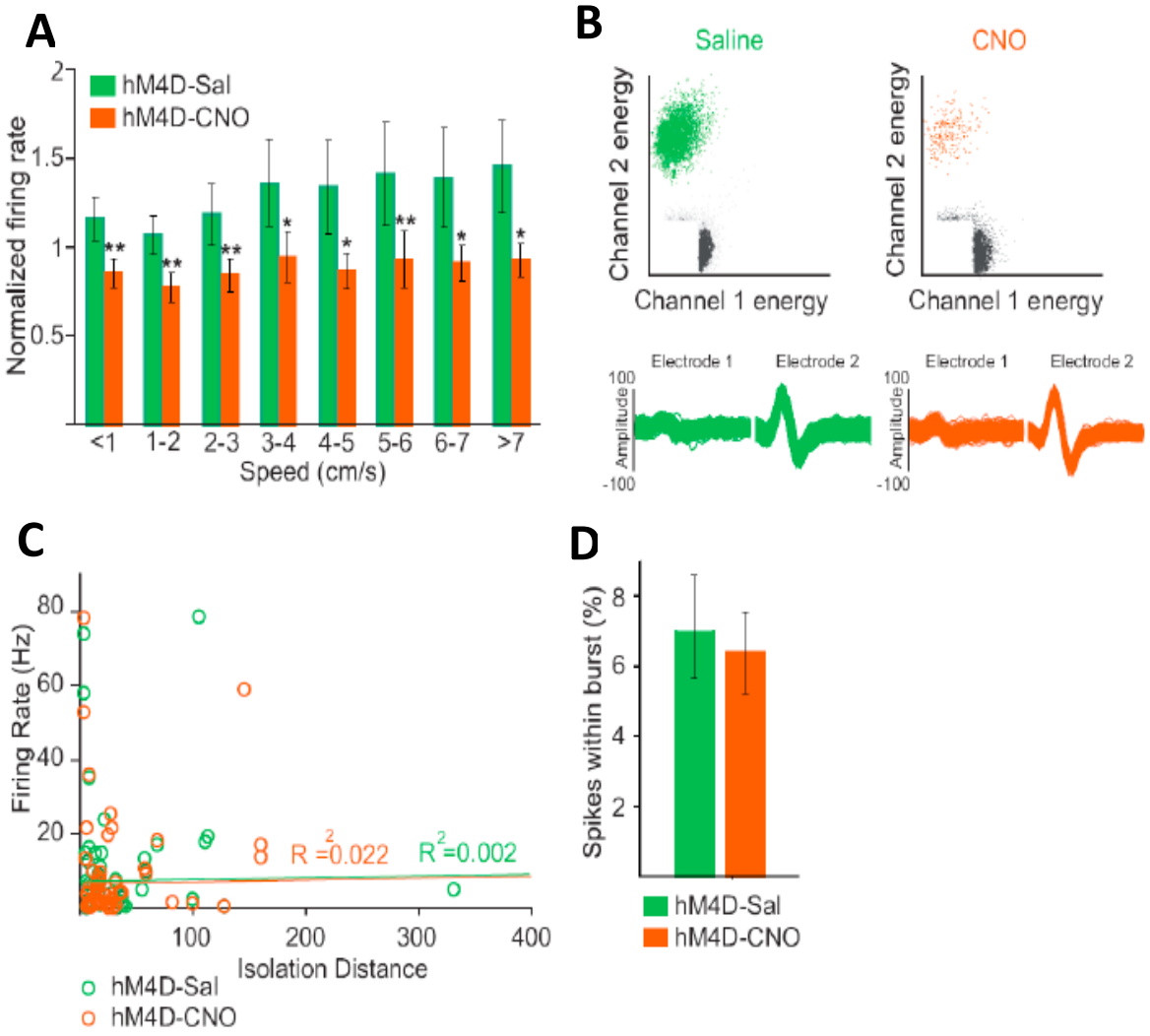

Figure 3.5 Quality of single unit isolation. A, The decrease in firing rate after CNO treatment is independent from the speed of the mice during recording (n=24; paired t-test, *p<0.05, **p<0.01). For each speed, the firing rate is normalized by the average firing rate during the whole session. **B,** Example of a clustered single-unit after saline-treatment (left, green) and after CNO-treatment (right, orange). On the bottom are the corresponding waveforms. **C,** The firing rates of the recorded 63 single-units do not correlate with the isolation distance (Correlation coefficient saline, green: R=0.04, CNO, orange: R=0.15). **D,** The percentage of spikes within burst events was not changed in CNO-treated MDhM4D mice compared to controls (number of cells n=40). Error bars: s.e.m.

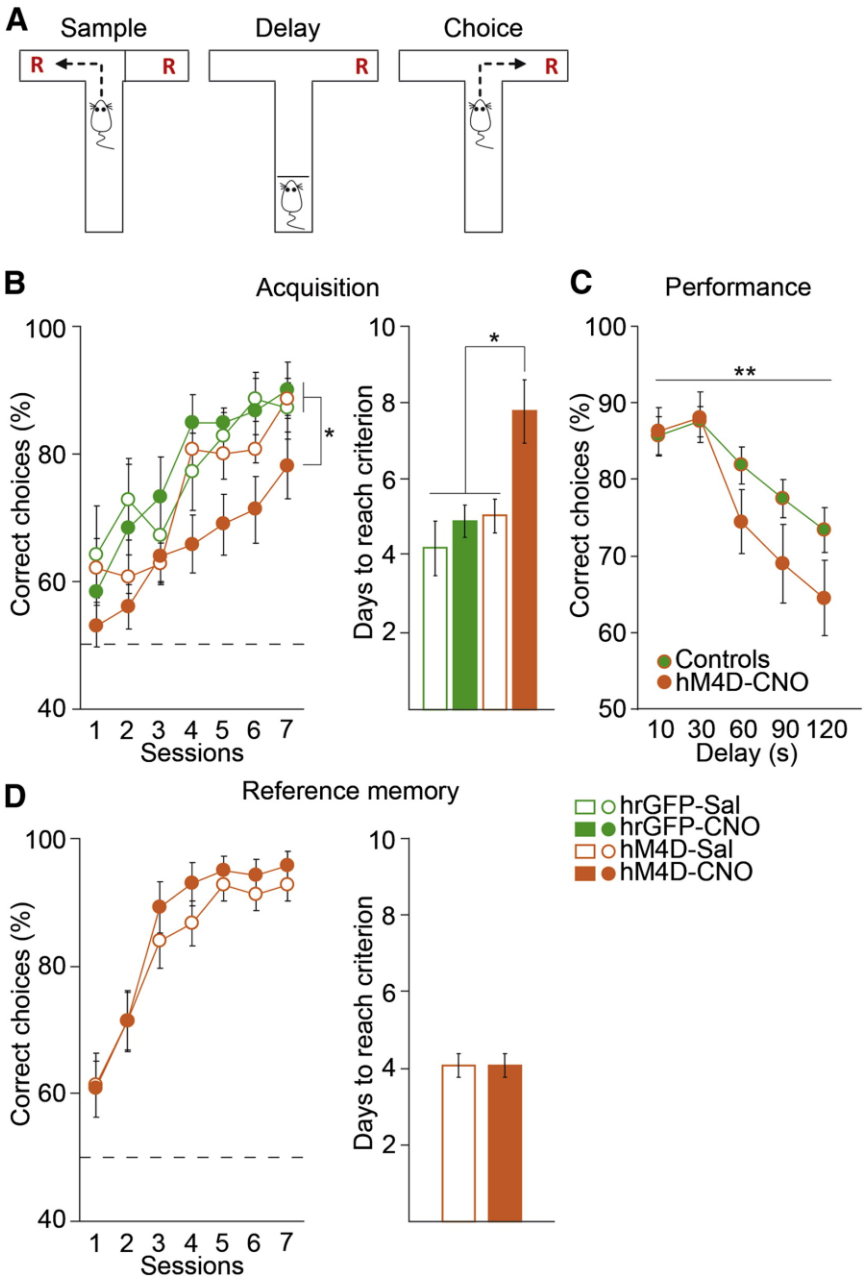

Figure 3.6 Decreasing Activity in the Mediodorsal Thalamus Leads to Deficits in Working Memory A, Task design for the T maze based DNMS working memory task. (R) depicts reward. **B,** CNO-treated MD_{hM4D} mice showed a deficit in acquisition (left panel) and took longer to reach criterion (right panel) compared to control groups (DNMS task) (ANOVA followed by Newman-Keuls post-hoc analysis $^{*}p < 0.05$; GFP-sal n = 7 GFP-CNO n = 6, hM4D-sal n = 12 and hM4D-CNO n = 11). **C,** CNO-treatment impaired DNMS performance on long delays in MD_{hM4D} mice after task acquisition (repeated-measures ANOVA, group effect $^{*}p < 0.05$; combined controls n = 21 including 5 GFP-sal, 4 GFP-CNO and 12 hM4D-sal; hM4D-CNO n = 11). **D,** Decreasing MD activity does not affect acquisition of a spatial reference memory T maze task (two-tailed t test p = 0.98; hM4D-sal n = 15 and hM4D-CNO n = 14).Error bars: SEM.

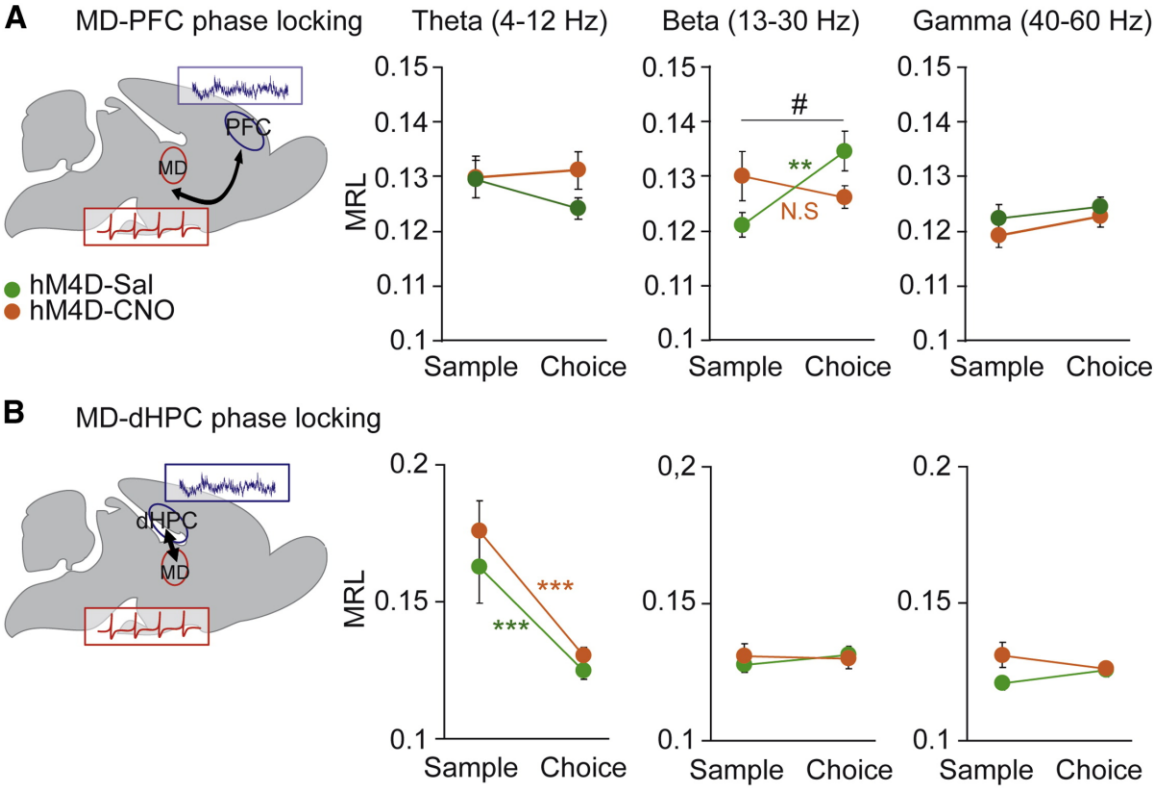

Figure 3.7. Enhancement of Thalamoprefrontal Beta Synchrony during Working Memory Performance Is Disrupted by Low MD Activity. A, Phase-locking of MD cells to mPFC LFP oscillations in the beta-, theta-, and gamma-frequency range as a function of task phase (sample versus choice) (repeated-measures ANOVA, group × task phase interaction #$p < 0.05$; hM4D-SAL cells n = 40 [green], hM4D-CNO cells n = 33 [orange]; sample-choice difference in controls, $^{**}p < 0.01$ by paired t test). **B,** Phase-locking of MD cells to dHPC LFP oscillations in the beta-, theta-, and gamma-frequency range as a function of task phase (sample versus choice) (paired t test sample-choice difference in controls and CNO-treated MD_{hM4D} mice, $^{***}p < 0.001$; hM4D-SAL cells n = 40 [green], hM4D-CNO cells n = 33 [orange]).

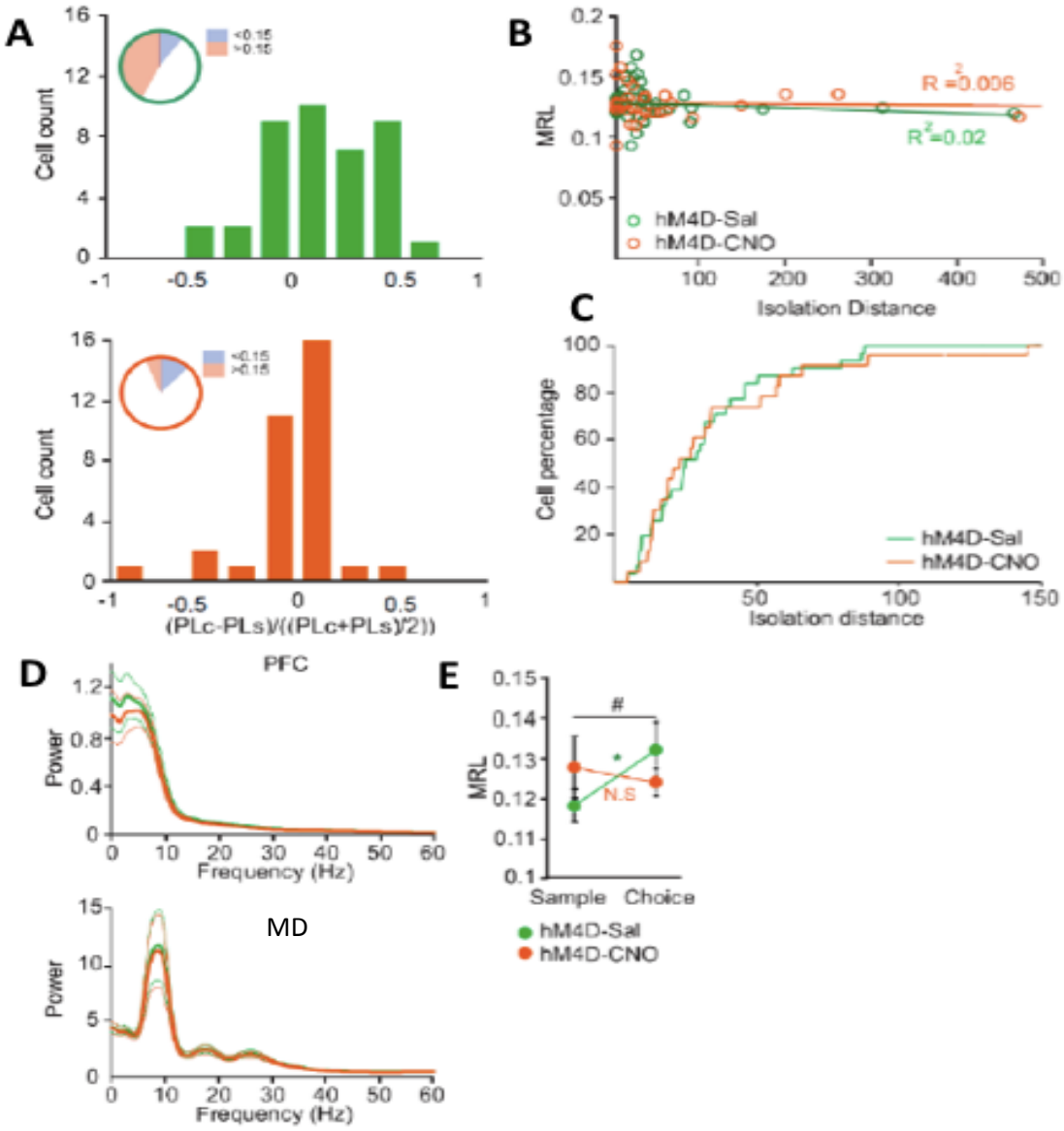

Figure 3.8 Supplemental analyses of MD phase locking to PFC beta-oscillations A, Histogram of the change of MD-PFC beta-phase locking between sample (PLs) and choice (PLc) phases in saline-(top, green; n=40) and CNO-treated (bottom, orange; n=33) MDhM4D mice. The pie charts represent the percentage of MD units that increased (>0.15; red), did not changed (white) or decreased (<-0.15; blue) their phase locking strength to PFC beta-oscillations. **B,** Phase-locking strength (MRL) does not correlate with isolation distance (Correlation coefficient saline, green: R=0.14, CNO, orange: R=0.077). **C,** Cumulative histogram of isolation distance after saline (green) or CNO treatment (orange); CNO had no effect on isolation distance. **D,** PFC (top) and MD (bottom) power spectra in saline- (green) and CNO-treated (orange) MDhM4D mice. **(E)** Phase locking of MD cells to PFC LFP oscillations in the beta-frequency range as a function of task phase in "CNO naive mice" (repeated ANOVA, group x task phase #p<0.05; hM4D-SAL cells n=10 (green), hM4D-CNO cells n=12 (orange); sample-choice difference in controls, *p < 0.05 by paired t-test).

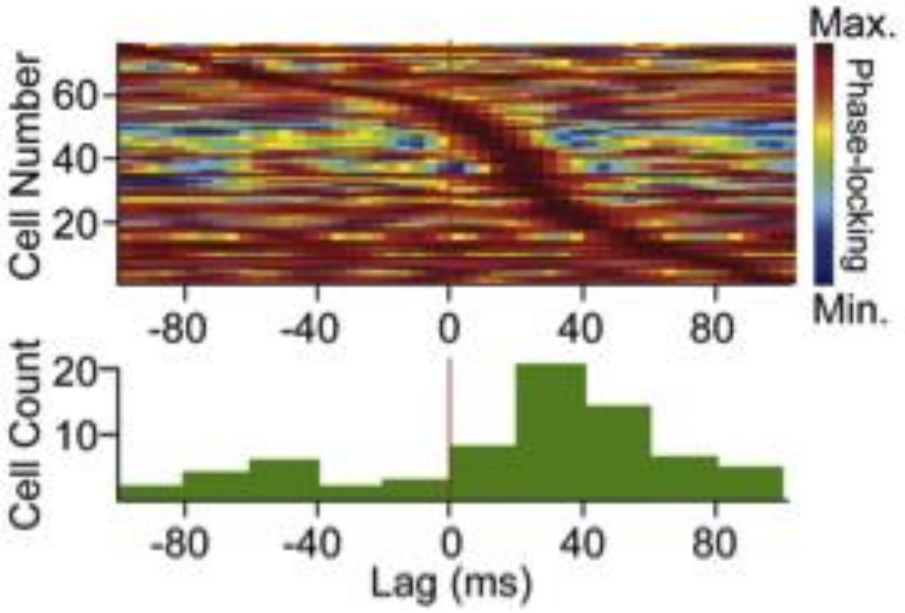

Figure 3.9 Activity of mediodorsal thalamus units leads mPFC beta oscillations. Upper panel, normalized beta-phase-locking strength as a function of lag to mPFC LFP for all MD cells with significant phase-locking to the mPFC, ordered by lag at which peak strength occurs. Bottom: distribution of lags at peak phase-locking strength (lag, +20 ± 1.4 ms, Wilcoxon signed-rank test $p < 0.05$, $n = 73$).

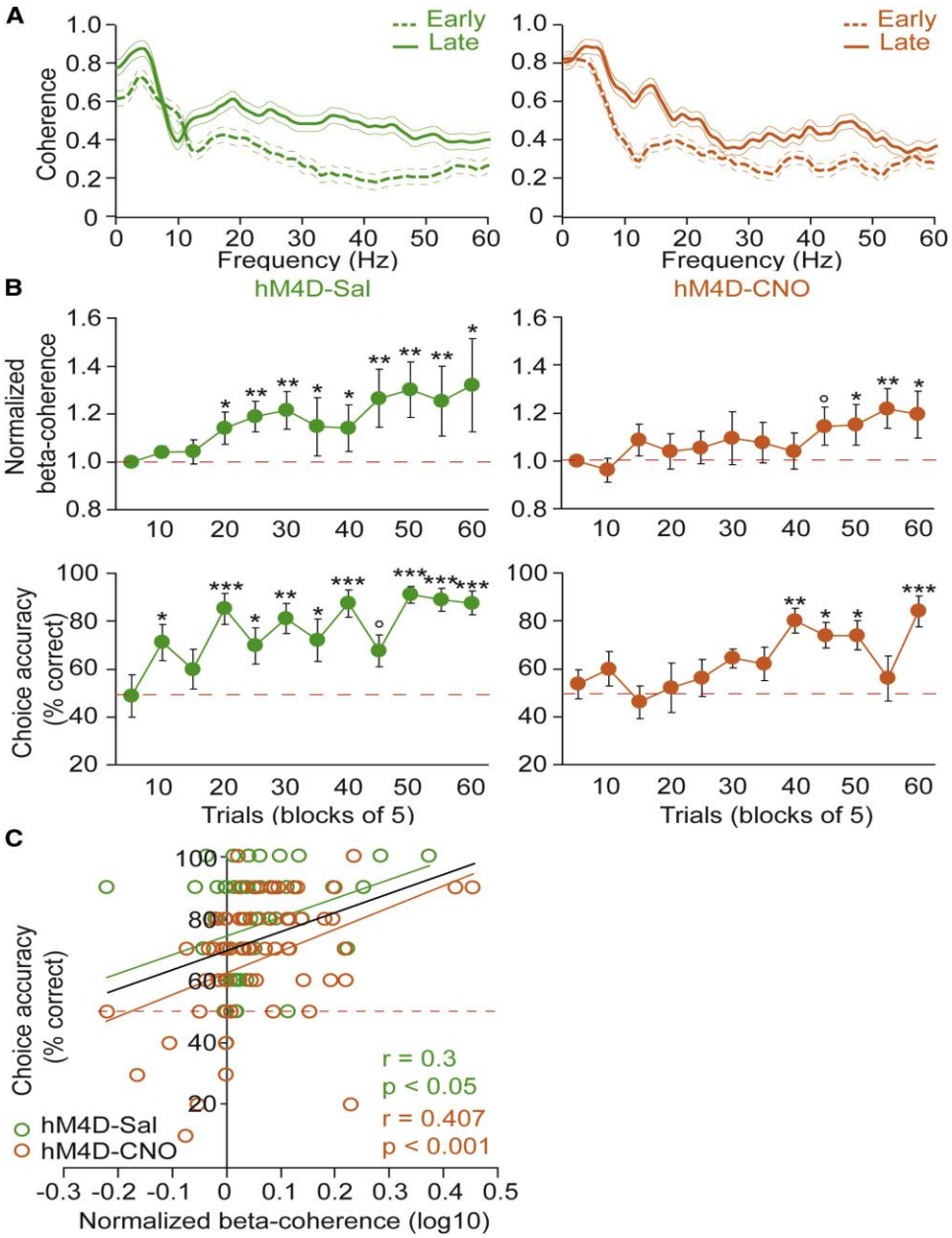

Figure 3.10 Synchronous Activity between Mediodorsal Thalamus and Prefrontal Cortex Correlates with Behavioral Performance in a Spatial Working Memory Task(A) Example of coherence spectra between early (trials 1–5; dashed lines) and late (5 last trials; solid lines) training phase in saline- (green) and CNO- (orange) treated MD_{hM4D} mice.(B) Time course of increases in MD-PFC beta coherence (top panels) and choice accuracy (bottom panels) in saline- (green, n = 9) and CNO- (orange, n = 10) treated MD_{hM4D} mice (repeated-measures ANOVA followed by Fischer post hoc analysis, difference versus trials 1–5, °p < 0.1 *p < 0.05, **p < 0.01, ***p < 0.001).(C) Correlation analysis between beta coherence and choice accuracy for each session (10 trials per session) in saline- (green) and CNO- (orange) treated MD_{hM4D} mice (Pearson correlation test, saline: correlation coefficient r = 0.3, p < 0.05, CNO: r = 0.407, p < 0.001).Error bars: SEM.

Chapter 4

Thesis Discussion

CHAPTER 4: THESIS DISCUSSION

4.1 Summary of principal findings

In the previous two chapters, we have presented data demonstrating that synchronous activity between the mPFC and two of its major anatomical inputs, the ventral region of the hippocampus and the medial dorsal thalamus, is modulated by the demands of a spatial working memory task. While it has previously been shown that the mPFC coordinates with the dorsal region of the hippocampus during working memory (Jones and Wilson 2005; Sigurdsson et al. 2010), these studies did not address the lack of an anatomical connection between the dHPC and the mPFC. Because functional connectivity must rely somewhat on anatomical connectivity, this is a non-trivial point. In Chapter 2, we tested whether the vHPC, which does have a robust axonal projection into the mPFC, could mediate dHPC-mPFC coherence. We first showed that characteristics of the mPFC and vHPC were significantly different from the dHPC in both power and peak frequency. This encouraged a hypothesis that mPFC may be paced by the vHPC input. Next, we showed that functional connectivity between the mPFC and vHPC, like dHPC-mPFC, increases with working memory demand. Specifically, theta power in the mPFC and vHPC was significantly more correlated during the choice phase of the task. Then, using a partial correlation technique, we demonstrated that removing the influence of the ventral hippocampus, dHPC-mPFC coherence decreased. In addition, inactivation of the vHPC with muscimol disrupted dHPC-mPFC synchrony while saline or a contralateral infusion of muscimol had no effect. Thus, the vHPC is involved in working memory and may play a role in behavior

through its mediation of dHPC-mPFC synchrony. This result is in line with previous disconnection studies (Floresco et al. 1997; Wang and Cai 2006) as their inactivation also targeted the vHPC. We did not observe, nor did we expect, an effect on behavior in our task as the contralateral HPC-mPFC circuit remained intact.

Reports on the MD-mPFC pathway during working memory are sparse. To start, lesion studies in rodents that test whether the MD is important in working memory do not agree with each other (Bailey and Mair 2005; Mitchell and Dalrymple-Alford 2005). This may be because the thalamus is comprised of many closely situated nuclei making it difficult to target only the MD with lesions or drug infusions while sparing the other regions. Nevertheless, motivated by findings from schizophrenia patients who exhibit decreased activity in the MD thalamus and abnormal PFC-MD connectivity during working memory, we were motivated to perform the set of experiments presented in Chapter 3: to selectively inactivate the MD and characterize any changes in working memory behavior and in the MD-mPFC activity. We found that the MD and mPFC do synchronize during the same spatial DNMS working memory task we used to assess vHPC-mPFC coordination. Specifically, phase-locking of MD cells to mPFC beta oscillations was significantly higher in the choice phase of the task. Our directionality analysis shows that the majority of significantly phase-locked MD cells do so to beta oscillations in the mPFC of the future, indicating that activity in the MD leads that of the mPFC. Using the DREADD system, we virally induced expression of hM4d in MD cells. Application of CNO led to hyperpolarization of hM4D-MD *in vitro* and a decrease (~30%) in firing rate in 30-60% of MD neurons *in vivo*. This subtle inactivation was sufficient to disrupt spatial working memory performance and abolish

the increase in MD-mPFC synchrony we had observed during task performance. In a separate cohort of animals we also tested the effect of MD inactivation on the animals' acquisition of the T-maze task. We observed that MD inactivated animals took longer than saline injected animals to acquire the task. Interestingly, MD-mPFC beta (and theta) coherence correlated with learning, suggesting that MD-mPFC synchrony is predictive of behavior.

4.2 Dorsal and ventral hippocampal functional differentiation

Several lines of evidence support the notion that the dorsal and ventral sub-regions of the hippocampus have dissociable functions (reviewed in Fanselow and Dong, 2010). First, anatomical studies report distinct input and output structures along the septo-temporal axis. The dHPC projects more strongly to structures involved in spatial representation such as the dorsal subiculum, that contains cells which code for the rodent's head position, and the anterior cingulate, which is involved in the processing of visuo-spatial information (Frankland et al. 2004; Jones and Wilson 2005). The vHPC, on the other hand, projects more to limbic areas such as the amygdala, which is crucial for fear learning, and to regions of the hypothalamus that are involved in motivated behaviors (Pitkanen et al. 2000). The entorhinal cortex, which provides the major input into the classic tri-synaptic hippocampal loop, sends afferents that are also segregated along the dorsal-ventral axis (Cenquizca and Swanson 2007).

Second, fitting with the distinction in anatomy, several groups have reported a functional differentiation along the HPC extent (Moser et al. 1993; Moser et al. 1995; Bannerman et al. 1999). Lesions of the ventral but not the dorsal HPC impaired expression of fear and led to

reduction in anxiety behavior (Kjelstrup et al. 2002; Bannerman et al. 2004). On the other hand, lesions of dHPC but not vHPC impaired performance in the Morris water maze, a task of spatial reference memory (Moser et al. 1995). This led to a proposal that the dHPC is associated with cognitive processes while the vHPC is more involved with emotional processes (Moser and Moser 1998). Nonetheless, as we'll now discuss, some datasets including our own demonstrate that this separation is not complete.

In another experiment to differentiate function between dHPC and vHPC in spatial reference memory, instead of placing the hidden platform in the same location across days, the researchers used a "one-trial match to position" version of the water maze in which the goal platform was moved at the start of each training day (Ferbinteanu et al. 2003). This adjustment, they argued, increased the spatial working memory demand, making the task more difficult for the rat. In contrast to the previous studies (Moser et al. 1993; Moser et al. 1995), vHPC lesions did impair performance on this task implying that the necessity of the vHPC is task-dependent (Ferbinteanu et al. 2003). Further, several other reports using reversible inactivation of the vHPC showed impairment in both performance of spatial reference (Floresco et al. 1996; Wang and Cai 2008) and spatial working memory tasks (Floresco et al. 1997; Wang and Cai 2006). The advantage of inactivation rather than lesion methods is the ability to assess different processes involved in learning and memory: acquisition, retention, retrieval, etc. With this technique, inactivation of either dHPC or vHPC after acquisition of a spatial reference memory was shown to impair the retrieval of that memory. In contrast, spatial memory can be acquired with either structure, though less efficiently with only the vHPC (Loureiro et al. 2012). This suggests that if a

memory is acquired with the entire HPC, the expression of that memory may also depend on the intact HPC.

Our results, that both ventral and dorsal HPC activity are synchronized with the mPFC during the choice phase of the T-maze, fit with the idea that the entire longitudinal axis of the HPC is engaged during spatial working memory behavior. Though we did not address the necessity of the vHPC, we suspect that had we inactivated the vHPC bilaterally after training, we would have seen a similar deficit to that observed in rats (Floresco, 1997; Wang and Cai, 2006).

The high theta coherence and power correlation we observed between dHPC and vHPC LFPs, regardless of task, suggest that they are highly coordinated in general. This may be due in part to intra-hippocampal projections between both principal cells and between principal cells and interneurons throughout the longitudinal extent of the HPC (Witter 2004). Furthermore, considering the basic structure of the tri-synaptic loop, DG to CA3 to CA1, this circuitry is conserved along the length of the HPC and therefore may reflect a common set of calculations during behavior. Indirect pathways common to the dHPC and vHPC could also facilitate their interaction. For example, the vHPC has a substantial projection to the perirhinal and postrhinal cortices, which provide afferents to the dHPC-associated region of the entorhinal cortex. Perhaps through this pathway, the rhinal cortices provide an integration point for vHPC and the visual/spatial information reaching the entorhinal cortex before this information is translated to the dHPC (Shi and Cassell 1999; Burwell 2000; Witter 2004).

Still, as the vHPC and dHPC sub regions are not completely dissociable, they are also not interchangeable. In addition to the studies we described above, further evidence for their distinction comes from place coding cells that are found in the both the dorsal and ventral HPC regions. While all place cells increase their firing rate according to the animal's location in space, vHPC place cells have broader spatial tuning than those in the dHPC (Jung et al. 1994; Kjelstrup et al. 2008; Royer et al. 2010). Thus, it is possible that the vHPC and dHPC may represent different aspects of the same context. Given the connection of the vHPC to limbic structures, it may represent more information about motivational or danger cues within the environment. In line with this, previous reports have shown that vHPC place cells tend to fire more near reward locations (Kjelstrup et al 2008). In contrast, the dHPC could represent more specific cues about the animal's moment to moment location.

4.3 Role of the vHPC input to mPFC in spatial working memory

The differentiation between ventral and dorsal poles may also be observed in their ability to coordinate with other structures such as the mPFC. Due to its anatomical projection to the mPFC, the vHPC would be expected to directly influence mPFC activity. Indeed, stimulation of vHPC in anesthetized rats has been shown to drive single unit activity (Tierney et al. 2004)and field responses (Laroche et al, 1990) within the mPFC. In awake, behaving rodents, both HPC regions have been shown to synchronize with the mPFC. Theta in the dHPC synchronizes both LFPs (Hyman et al; 2005) and cells in the mPFC (Siapas, 2005). This synchrony becomes greater with the demands of a working memory task (Chapter 2; Jones and Wilson, 2005; Sigurdsson

2010) though this effect could also be due to increases in attention. Likewise, we showed that theta oscillations in the vHPC increase in synchrony with the mPFC during the same task. A concern in recording LFPs is that the signal from one area can be due to contamination by another signal. While we cannot fully rule this out, the vHPC and dHPC are not likely to be the same signal as they vary from one another in power and peak frequency (Chapter 2). In addition, another study from our lab has shown mPFC units and LFPs differentially synchronize to ventral versus dorsal HPC, which would not likely be the case if the dorsal and ventral signals were similar (Adhikari, 2010). Our results from Chapter 2 indicate that dHPC-mPFC synchrony observed in previous studies may be mediated by the vHPC. Removing the influence of the vHPC mathematically resulted in a reduction of dHPC-mPFC coherence and abolished an increase in dHPC-mPFC synchrony during the T maze task. In addition, infusing a small volume of muscimol into the vHPC had no effect on the ability of vHPC to coordinate with the mPFC or the dHPC but was sufficient to cause a significant reduction in dHPC-mPFC coherence. It is important to note that these results do not exclude the possibility that another structure connected to both the dHPC and mPFC could mediate their interaction.

Aside from a role as mediator, the vHPC may itself be crucial in influencing mPFC activity. It has recently been shown in rats that during a decision making task, cells in the mPFC synchronize with vHPC theta as a new rule is acquired (Benchenane et al, 2010). Notably, units that became more phase-locked to the vHPC during this time also became more correlated with one another, suggesting that the vHPC can influence the formation of local ensembles in the mPFC. This is an intriguing result because the exact neural processes within the rodent mPFC during

working memory performance are incompletely understood and individual mPFC neurons display a diversity of task-related firing patterns (Jung et al. 1998). The study by Benchenane et al, demonstrates that the representation of a cognitive process within the mPFC may be revealed in the network of co active units, recruited by the vHPC or other structure, rather than on a single cell basis.

The vHPC-mPFC pathway is not only associated with cognitive behaviors but has recently been implicated in anxiety-like behavior as well. One study from our group showed that LFPs and units in the mPFC were more coherent with theta oscillations in the vHPC as mice navigated an anxiogenic as compared to a familiar environment (Adhikari et al. 2010; Adhikari et al. 2011). Some of the recorded units were task-related meaning and would differentially fire in anxiogenic versus safe environments. Interestingly, these task-related cells were more likely to phase lock to vHPC while modulation of mPFC-dHPC coherence was negligible throughout. The vHPC may therefore have a more varied role in behavior than the dHPC in that it seems to be involved in both cognitive and emotional processes. Input from the vHPC could differentially recruit mPFC units depending on the task at hand to then select the appropriate behavioral response.

Further investigation of the specific role of the vHPC input to mPFC would require the use of techniques such as optogenetics to silence inputs of the vHPC to the mPFC in both anxiety and working memory tasks. While this has recently been shown to disrupt spatial working memory

behavior, effects on activity within the mPFC or on dHPC-mPFC synchrony are not yet known (Rosen and Spellman et al, 2013 submitted).

4.4 Role of the MD in spatial working memory

As far as we know, our results are the first to demonstrate a causal role for the MD in functional cognition and to propose a mechanism for MD-mPFC coordination during a spatial memory task. Previous studies that implicated the MD in cognitive processes of rodents were often large lesions that damaged multiple midline nuclei, thus deficits could not be attributed specifically to the MD (Bailey and Mair 2005; Mitchell and Dalrymple-Alford 2005). In our experiment, we showed that even a subtle decrease in firing rate in a small population of MD units disrupted behavior in the T-maze. The observation that both acquisition and performance were affected highlights the important role of the MD in both processes.

The MD is highly interconnected with cortical, limbic and motor structures, which could provide it a central role in linking these pathways during behavior. Through its input from the substantia nigra and ventral pallidum, the MD receives input from the striatal reward circuit. The thalamus, in general, is a major output structure of the basal ganglia motor pathway, with the MD receiving substantial input from the globus pallidus. In addition, while it is not directly connected to the HPC, the MD receives afferents from the entorhinal cortex, which could support memory-related functions within the MD. Given its connectivity with these numerous

cortical and subcortical structures it should not be surprising that the MD has been implicated in multiple cognitive processes.

In monkeys, the MD exhibits sustained neuronal activation in the delay phase of delayed match to sample or visual recognition tasks (Fuster and Alexander 1973; Fahy et al. 1993). In addition, there is a predominance of neurons that respond selectively to stimulus location during spatial working memory (Goldman-Rakic et al. 1990). We observed some task related modulation of MD cells in mice during the T maze but these were not significantly affected by CNO. Therefore, the precise role of MD cell activity during the T maze DNMS working memory task is yet unclear and will be a topic of exploration in the near future.

Interestingly, our results regarding MD-mPFC synchrony highlighted oscillations in the beta-frequency band. The network mechanisms that generate beta oscillations are not known. However, GABA-ergic neurons in the globus pallidus have been shown to display intrinsic oscillatory properties (Nambu and Llinas 1994; Stanford 2003) and, through reciprocal interactions with the subthalamic nucleus, could support beta oscillatory activity within the entire basal ganglia network (Mallet et al. 2008). Functionally, beta-band activity has been found in relation to motor functions (review in Engel and Fries, 2010) and has been recorded within the entire motor system (the motor cortex basal ganglia, peripheral motor units, and cerebellum). In these studies, beta activity decreases during movement and is highest in the holding periods after movement; an 'akinetic' signal. In line with this, Parkinson's patients exhibit a disruption in movement initiation that is accompanied by excessive beta oscillatory activity in the basal ganglia (Nini et al. 1995; Bergman et al. 1998). A slight variation on this view

(Engel and Fries 2010) proposes a role for beta activity as a maintenance signal that represents the current sensory motor state of an animal. Beta coherence between MD and the mPFC could therefore reflect the maintenance of pertinent movement related information useful for performing in cognitive tasks. In this context, while more often associated with motor behaviors, beta band activity in humans and monkeys has also been shown to increase during visual and prefrontal cortices during working memory tasks (Siegel et al, 2009; Tallon-Baudry, 2004; Deiber et al 2007).

4.5 Theta vs. Beta frequencies during spatial working memory

In our experiments, synchrony between the mPFC-HPC and MD-mPFC was modulated predominantly in the theta and beta frequencies, respectively. Whether these two frequency bands are functionally separable and/or if they interact during spatial working memory is still unclear. Studies in the rodent HPC have focused on two frequency modes of synchronization: theta and gamma. Because slow oscillations have long conductions delays, theta frequency activity is thought to support a connection between structures that are relatively far apart. Coordination in the theta range has been reported between the HPC and several associated structures: the mPFC in working memory (Jones and Wilson 2005), the amygdala during fear memory retrieval (Seidenbecher et al. 2003) and the striatum during a procedural task (DeCoteau et al. 2007). Fast oscillations, on the other hand, have been shown to synchronize local network activity (Csicsvari et al. 2003).

There is now a growing body of evidence that interaction between different frequencies of oscillation, namely the phase or amplitude modulation of fast by slow oscillations, may be important in the facilitation of communication between brain regions. Gamma oscillations within both the mPFC and the HPC have been found to phase lock to theta oscillations in the HPC (Sirota et al. 2008; Colgin et al. 2009). This functional relevance of theta-gamma coupling is still not clear though some studies have shown an increase in theta modulated gamma during item-context association learning (Tort et al. 2009), and during performance on a working memory task (Li et al. 2012). While cross-frequency modulation has been shown mostly in theta-gamma coupling, the same could be true for beta-gamma coordination or perhaps theta-beta coordination. For example, coupling of both beta and gamma amplitude oscillations to theta phase was more pronounced during successful working memory maintenance in humans (Axmacher et al. 2010). The role of cross frequency coupling within and between structures in our behavioral task will be an interesting new avenue to explore.

Taken together, our data suggests that inputs into the mPFC from both the MD and the vHPC are necessary during a working memory task though they may represent different aspects of the task. The MD, through its connections with the basal ganglia may provide the mPFC with information about the animal's movement through the Tmaze. This is seen as an increase in coherence in the beta frequency range, as schematized below. The vHPC, through its connection to limbic structures and the dHPC may provide the mPFC with contextual, reward-related information primarily in the theta frequency range. Because there is no direct anatomical connection between the MD and the HPC, these two structures may converge in the

mPFC where they could activate cells ensembles that lead to successful behavior in a working memory task.

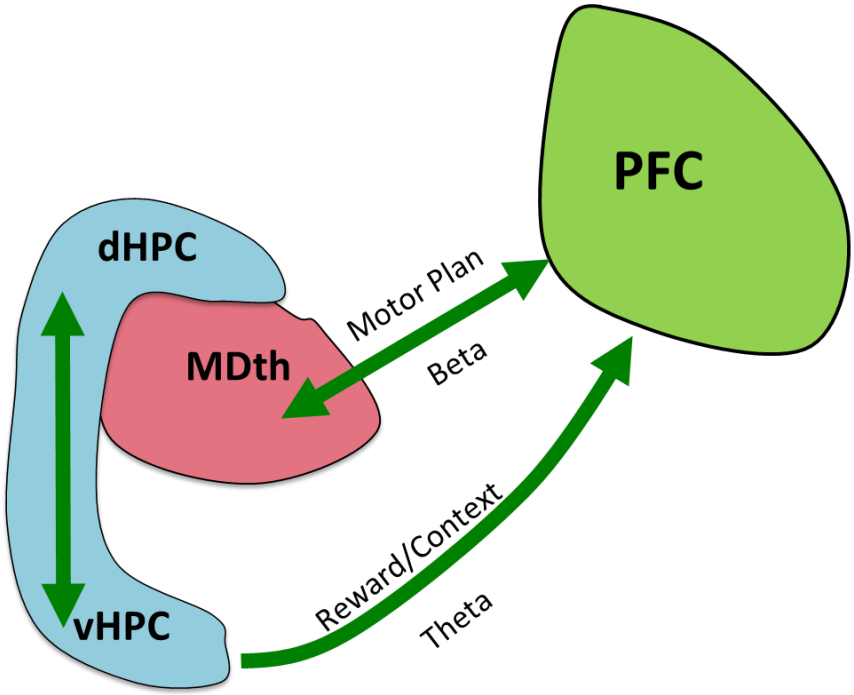

4.6 Conclusion

The precise circuit mechanisms that are involved in spatial working memory behavior are yet to be understood. By measuring the dynamic coordination within and between several brain regions, we can begin to associate more specific neural correlates to more specific cognitive processes. This thesis has explored the mechanisms by which the mPFC-HPC and MD-mPFC circuits coordinate during spatial working memory, but many other brain regions are also involved. Nonetheless, we hope that using these types of approaches, we will be able to form a more complete understanding of the neural circuits that underlie functional and dysfunctional working memory behavior.

REFERENCES

Addington, J. and D. Addington (2000). "Neurocognitive and social functioning in schizophrenia: a 2.5 year follow-up study." Schizophr Res **44**(1): 47-56.

Adhikari, A., M. A. Topiwala, et al. (2010). "Synchronized activity between the ventral hippocampus and the medial prefrontal cortex during anxiety." Neuron **65**(2): 257-269.

Adhikari, A., M. A. Topiwala, et al. (2011). "Single units in the medial prefrontal cortex with anxiety-related firing patterns are preferentially influenced by ventral hippocampal activity." Neuron **71**(5): 898-910.

Alexander, G. M., S. C. Rogan, et al. (2009). "Remote control of neuronal activity in transgenic mice expressing evolved G protein-coupled receptors." Neuron **63**(1): 27-39.

Andreasen, N. C., K. Rezai, et al. (1992). "Hypofrontality in neuroleptic-naive patients and in patients with chronic schizophrenia. Assessment with xenon 133 single-photon emission computed tomography and the Tower of London." Arch Gen Psychiatry **49**(12): 943-958.

Andrews, J., L. Wang, et al. (2006). "Abnormalities of thalamic activation and cognition in schizophrenia." Am J Psychiatry **163**(3): 463-469.

Armbruster, B. N., X. Li, et al. (2007). "Evolving the lock to fit the key to create a family of G protein-coupled receptors potently activated by an inert ligand." Proc Natl Acad Sci U S A **104**(12): 5163-5168.

Association, A. P. (2000). Diagnostic and statistical manual of mental disorders. **4th ed., text rev.**

Axmacher, N., M. M. Henseler, et al. (2010). "Cross-frequency coupling supports multi-item working memory in the human hippocampus." Proc Natl Acad Sci U S A **107**(7): 3228-3233.

Baare, W. F., H. E. Hulshoff Pol, et al. (1999). "Volumetric analysis of frontal lobe regions in schizophrenia: relation to cognitive function and symptomatology." Biol Psychiatry **45**(12): 1597-1605.

Baddeley, A. (1992). "Working memory." Science **255**(5044): 556-559.

Bailey, K. R. and R. G. Mair (2005). "Lesions of specific and nonspecific thalamic nuclei affect prefrontal cortex-dependent aspects of spatial working memory." Behav Neurosci **119**(2): 410-419.

Bannerman, D. M., J. N. Rawlins, et al. (2004). "Regional dissociations within the hippocampus--memory and anxiety." Neurosci Biobehav Rev **28**(3): 273-283.

Bannerman, D. M., B. K. Yee, et al. (1999). "Double dissociation of function within the hippocampus: a comparison of dorsal, ventral, and complete hippocampal cytotoxic lesions." Behav Neurosci **113**(6): 1170-1188.

Barch, D. M., C. S. Carter, et al. (2001). "Selective deficits in prefrontal cortex function in medication-naive patients with schizophrenia." Arch Gen Psychiatry **58**(3): 280-288.

Bechara, A., H. Damasio, et al. (1998). "Dissociation Of working memory from decision making within the human prefrontal cortex." J Neurosci **18**(1): 428-437.

Benchenane, K., A. Peyrache, et al. (2010). "Coherent theta oscillations and reorganization of spike timing in the hippocampal- prefrontal network upon learning." Neuron **66**(6): 921-936.

Beracochea, D. J., R. Jaffard, et al. (1989). "Effects of anterior or dorsomedial thalamic ibotenic lesions on learning and memory in rats." Behav Neural Biol **51**(3): 364-376.

Bergman, H., A. Feingold, et al. (1998). "Physiological aspects of information processing in the basal ganglia of normal and parkinsonian primates." Trends Neurosci **21**(1): 32-38.

Blatow, M., A. Rozov, et al. (2003). "A novel network of multipolar bursting interneurons generates theta frequency oscillations in neocortex." Neuron **38**(5): 805-817.

Boutros, N. N., C. Arfken, et al. (2008). "The status of spectral EEG abnormality as a diagnostic test for schizophrenia." Schizophr Res **99**(1-3): 225-237.

Bowie, C. R., A. Reichenberg, et al. (2006). "Determinants of real-world functional performance in schizophrenia subjects: correlations with cognition, functional capacity, and symptoms." Am J Psychiatry **163**(3): 418-425.

Burwell, R. D. (2000). "The parahippocampal region: corticocortical connectivity." Ann N Y Acad Sci **911**: 25-42.

Buzsaki, G. (2002). "Theta oscillations in the hippocampus." Neuron **33**(3): 325-340.

Buzsaki, G. (2004). "Large-scale recording of neuronal ensembles." Nat Neurosci **7**(5): 446-451.

Buzsaki, G., C. A. Anastassiou, et al. (2012). "The origin of extracellular fields and currents--EEG, ECoG, LFP and spikes." Nat Rev Neurosci **13**(6): 407-420.

Byne, W., E. A. Hazlett, et al. (2009). "The thalamus and schizophrenia: current status of research." Acta Neuropathol **117**(4): 347-368.

Cenquizca, L. A. and L. W. Swanson (2007). "Spatial organization of direct hippocampal field CA1 axonal projections to the rest of the cerebral cortex." Brain Res Rev **56**(1): 1-26.

Colgin, L. L. (2011). "Oscillations and hippocampal-prefrontal synchrony." Curr Opin Neurobiol **21**(3): 467-474.

Colgin, L. L., T. Denninger, et al. (2009). "Frequency of gamma oscillations routes flow of information in the hippocampus." Nature **462**(7271): 353-357.

Csicsvari, J., B. Jamieson, et al. (2003). "Mechanisms of gamma oscillations in the hippocampus of the behaving rat." Neuron **37**(2): 311-322.

Dalley, J. W., R. N. Cardinal, et al. (2004). "Prefrontal executive and cognitive functions in rodents: neural and neurochemical substrates." Neurosci Biobehav Rev **28**(7): 771-784.

DeCoteau, W. E., C. Thorn, et al. (2007). "Learning-related coordination of striatal and hippocampal theta rhythms during acquisition of a procedural maze task." Proc Natl Acad Sci U S A **104**(13): 5644-5649.

Degenetais, E., A. M. Thierry, et al. (2003). "Synaptic influence of hippocampus on pyramidal cells of the rat prefrontal cortex: an in vivo intracellular recording study." Cereb Cortex **13**(7): 782-792.

Deiber, M. P., P. Missonnier, et al. (2007). "Distinction between perceptual and attentional processing in working memory tasks: a study of phase-locked and induced oscillatory brain dynamics." J Cogn Neurosci **19**(1): 158-172.

Dembrow, N. C., D. L. Pettit, et al. (2010). "Calcium dynamics encode the magnitude of a graded memory underlying sensorimotor adaptation." J Neurophysiol **103**(5): 2372-2381.

Dias, R. and J. P. Aggleton (2000). "Effects of selective excitotoxic prefrontal lesions on acquisition of nonmatching- and matching-to-place in the T-maze in the rat: differential involvement of the prelimbic-infralimbic and anterior cingulate cortices in providing behavioural flexibility." Eur J Neurosci **12**(12): 4457-4466.

Dolleman-van der Weel, M. J., R. G. Morris, et al. (2009). "Neurotoxic lesions of the thalamic reuniens or mediodorsal nucleus in rats affect non-mnemonic aspects of watermaze learning." Brain Struct Funct **213**(3): 329-342.

Dudchenko, P. A. (2001). "How do animals actually solve the T maze?" Behav Neurosci **115**(4): 850-860.

Dunnett, S. B. (1990). "Role of prefrontal cortex and striatal output systems in short-term memory deficits associated with ageing, basal forebrain lesions, and cholinergic-rich grafts." Can J Psychol **44**(2): 210-232.

Ellison-Wright, I. and E. Bullmore (2009). "Meta-analysis of diffusion tensor imaging studies in schizophrenia." Schizophr Res **108**(1-3): 3-10.

Engel, A. K. and P. Fries (2010). "Beta-band oscillations--signalling the status quo?" Curr Opin Neurobiol **20**(2): 156-165.

Eslinger, P. J. and A. R. Damasio (1985). "Severe disturbance of higher cognition after bilateral frontal lobe ablation: patient EVR." Neurology **35**(12): 1731-1741.

Fahy, F. L., I. P. Riches, et al. (1993). "Neuronal signals of importance to the performance of visual recognition memory tasks: evidence from recordings of single neurones in the medial thalamus of primates." Prog Brain Res **95**: 401-416.

Fanselow, M. S. and H. W. Dong (2010). "Are the dorsal and ventral hippocampus functionally distinct structures?" Neuron **65**(1): 7-19.

Ferbinteanu, J., C. Ray, et al. (2003). "Both dorsal and ventral hippocampus contribute to spatial learning in Long-Evans rats." Neurosci Lett **345**(2): 131-135.

Floresco, S. B., D. N. Braaksma, et al. (1999). "Thalamic-cortical-striatal circuitry subserves working memory during delayed responding on a radial arm maze." J Neurosci **19**(24): 11061-11071.

Floresco, S. B., J. K. Seamans, et al. (1996). "Differential effects of lidocaine infusions into the ventral CA1/subiculum or the nucleus accumbens on the acquisition and retention of spatial information." Behav Brain Res **81**(1-2): 163-171.

Floresco, S. B., J. K. Seamans, et al. (1997). "Selective roles for hippocampal, prefrontal cortical, and ventral striatal circuits in radial-arm maze tasks with or without a delay." J Neurosci **17**(5): 1880-1890.

Ford, J. M., D. H. Mathalon, et al. (2002). "Reduced communication between frontal and temporal lobes during talking in schizophrenia." Biol Psychiatry **51**(6): 485-492.

Frankland, P. W., B. Bontempi, et al. (2004). "The involvement of the anterior cingulate cortex in remote contextual fear memory." Science **304**(5672): 881-883.

Freedman, M. and M. Oscar-Berman (1986). "Bilateral frontal lobe disease and selective delayed response deficits in humans." Behav Neurosci **100**(3): 337-342.

Fries, P. (2005). "A mechanism for cognitive dynamics: neuronal communication through neuronal coherence." Trends Cogn Sci **9**(10): 474-480.

Friston, K. J. (1998). "The disconnection hypothesis." Schizophr Res **30**(2): 115-125.

Funahashi, S., C. J. Bruce, et al. (1993). "Dorsolateral prefrontal lesions and oculomotor delayed-response performance: evidence for mnemonic "scotomas"." J Neurosci **13**(4): 1479-1497.

Funahashi, S., M. Inoue, et al. (1993). "Delay-related activity in the primate prefrontal cortex during sequential reaching tasks with delay." Neurosci Res **18**(2): 171-175.

Funahashi, S. and K. Kubota (1994). "Working memory and prefrontal cortex." Neurosci Res **21**(1): 1-11.

Fuster, J. M. (1973). "Unit activity in prefrontal cortex during delayed-response performance: neuronal correlates of transient memory." J Neurophysiol **36**(1): 61-78.

Fuster, J. M. and G. E. Alexander (1973). "Firing changes in cells of the nucleus medialis dorsalis associated with delayed response behavior." Brain Res **61**: 79-91.

Garner, A. R., D. C. Rowland, et al. (2012). "Generation of a synthetic memory trace." Science **335**(6075): 1513-1516.

Gevins, A., M. E. Smith, et al. (1997). "High-resolution EEG mapping of cortical activation related to working memory: effects of task difficulty, type of processing, and practice." Cereb Cortex **7**(4): 374-385.

Goldberg, T. E. and D. R. Weinberger (1996). "Effects of neuroleptic medications on the cognition of patients with schizophrenia: a review of recent studies." J Clin Psychiatry **57 Suppl 9**: 62-65.

Goldman-Rakic, P. S., M. S. Lidow, et al. (1990). "Overlap of dopaminergic, adrenergic, and serotoninergic receptors and complementarity of their subtypes in primate prefrontal cortex." J Neurosci **10**(7): 2125-2138.

Gordon, J. A. (2011). "Oscillations and hippocampal-prefrontal synchrony." Curr Opin Neurobiol **21**(3): 486-491.

Grastyan, E., K. Lissak, et al. (1959). "Hippocampal electrical activity during the development of conditioned reflexes." Electroencephalogr Clin Neurophysiol **11**(3): 409-430.

Gray, C. M. and W. Singer (1989). "Stimulus-specific neuronal oscillations in orientation columns of cat visual cortex." Proc Natl Acad Sci U S A **86**(5): 1698-1702.

Green, M. F., R. S. Kern, et al. (2000). "Neurocognitive deficits and functional outcome in schizophrenia: are we measuring the "right stuff"?" Schizophr Bull **26**(1): 119-136.

Green, M. F., S. R. Marder, et al. (2002). "The neurocognitive effects of low-dose haloperidol: a two-year comparison with risperidone." Biol Psychiatry **51**(12): 972-978.

Guettier, J. M., D. Gautam, et al. (2009). "A chemical-genetic approach to study G protein regulation of beta cell function in vivo." Proc Natl Acad Sci U S A **106**(45): 19197-19202.

Haber, S. N. and R. Calzavara (2009). "The cortico-basal ganglia integrative network: the role of the thalamus." Brain Res Bull **78**(2-3): 69-74.

Haenschel, C., R. A. Bittner, et al. (2007). "Contribution of impaired early-stage visual processing to working memory dysfunction in adolescents with schizophrenia: a study with event-related potentials and functional magnetic resonance imaging." Arch Gen Psychiatry **64**(11): 1229-1240.

Hampson, R. E., J. D. Simeral, et al. (1999). "Distribution of spatial and nonspatial information in dorsal hippocampus." Nature **402**(6762): 610-614.

Harrison, L. M. and R. G. Mair (1996). "A comparison of the effects of frontal cortical and thalamic lesions on measures of spatial learning and memory in the rat." Behav Brain Res **75**(1-2): 195-206.

Haupt, M., J. A. Eccard, et al. (2010). "Does spatial learning ability of common voles (Microtus arvalis) and bank voles (Myodes glareolus) constrain foraging efficiency?" Anim Cogn **13**(6): 783-791.

Heckers, S. (1997). "Neuropathology of schizophrenia: cortex, thalamus, basal ganglia, and neurotransmitter-specific projection systems." Schizophr Bull **23**(3): 403-421.

Hembrook, J. R., K. D. Onos, et al. (2012). "Inactivation of ventral midline thalamus produces selective spatial delayed conditional discrimination impairment in the rat." Hippocampus **22**(4): 853-860.

Hoover, W. B. and R. P. Vertes (2007). "Anatomical analysis of afferent projections to the medial prefrontal cortex in the rat." Brain Struct Funct **212**(2): 149-179.

Hoover, W. B. and R. P. Vertes (2012). "Collateral projections from nucleus reuniens of thalamus to hippocampus and medial prefrontal cortex in the rat: a single and double retrograde fluorescent labeling study." Brain Struct Funct **217**(2): 191-209.

Hornak, J., J. O'Doherty, et al. (2004). "Reward-related reversal learning after surgical excisions in orbito-frontal or dorsolateral prefrontal cortex in humans." J Cogn Neurosci **16**(3): 463-478.

Hunt, P. R. and J. P. Aggleton (1991). "Medial dorsal thalamic lesions and working memory in the rat." Behav Neural Biol **55**(2): 227-246.

Hunt, P. R. and J. P. Aggleton (1998). "Neurotoxic lesions of the dorsomedial thalamus impair the acquisition but not the performance of delayed matching to place by rats: a deficit in shifting response rules." J Neurosci **18**(23): 10045-10052.

Hyman, J. M., E. A. Zilli, et al. (2010). "Working Memory Performance Correlates with Prefrontal-Hippocampal Theta Interactions but not with Prefrontal Neuron Firing Rates." Front Integr Neurosci **4**: 2.

Izaki, Y., M. Takita, et al. (2008). "Specific role of the posterior dorsal hippocampus-prefrontal cortex in short-term working memory." Eur J Neurosci **27**(11): 3029-3034.

Jacobsen, C. F. (1935). "Functions of frontal association area in primates." Arch Neurol Psychiatry **33**: 558-569.

Jahnsen, H. and R. Llinas (1984). "Ionic basis for the electro-responsiveness and oscillatory properties of guinea-pig thalamic neurones in vitro." J Physiol **349**: 227-247.

Jann, M. W., Y. W. Lam, et al. (1994). "Rapid formation of clozapine in guinea-pigs and man following clozapine-N-oxide administration." Arch Int Pharmacodyn Ther **328**(2): 243-250.

Jones, E. G. (2007). The Thalamus. New York, Cambridge University Press.

Jones, M. W. and M. A. Wilson (2005). "Theta rhythms coordinate hippocampal-prefrontal interactions in a spatial memory task." PLoS Biol **3**(12): e402.

Jonides, J., E. E. Smith, et al. (1993). "Spatial working memory in humans as revealed by PET." Nature **363**(6430): 623-625.

Jouvet, M. (1969). "Biogenic amines and the states of sleep." Science **163**(3862): 32-41.

Jung, M. W., S. I. Wiener, et al. (1994). "Comparison of spatial firing characteristics of units in dorsal and ventral hippocampus of the rat." J Neurosci **14**(12): 7347-7356.

Keefe, R. S., S. G. Silva, et al. (1999). "The effects of atypical antipsychotic drugs on neurocognitive impairment in schizophrenia: a review and meta-analysis." Schizophr Bull **25**(2): 201-222.

Kellendonk, C., E. H. Simpson, et al. (2006). "Transient and selective overexpression of dopamine D2 receptors in the striatum causes persistent abnormalities in prefrontal cortex functioning." Neuron **49**(4): 603-615.

Kesner, R. P., M. E. Hunt, et al. (1996). "Prefrontal cortex and working memory for spatial response, spatial location, and visual object information in the rat." Cereb Cortex **6**(2): 311-318.

Kisley, M. A. and Z. M. Cornwell (2006). "Gamma and beta neural activity evoked during a sensory gating paradigm: effects of auditory, somatosensory and cross-modal stimulation." Clin Neurophysiol **117**(11): 2549-2563.

Kjelstrup, K. B., T. Solstad, et al. (2008). "Finite scale of spatial representation in the hippocampus." Science **321**(5885): 140-143.

Kjelstrup, K. G., F. A. Tuvnes, et al. (2002). "Reduced fear expression after lesions of the ventral hippocampus." Proc Natl Acad Sci U S A **99**(16): 10825-10830.

Klimesch, W. (1999). "EEG alpha and theta oscillations reflect cognitive and memory performance: a review and analysis." Brain Res Brain Res Rev **29**(2-3): 169-195.

Kuroda, M., J. Yokofujita, et al. (1998). "An ultrastructural study of the neural circuit between the prefrontal cortex and the mediodorsal nucleus of the thalamus." Prog Neurobiol **54**(4): 417-458.

Laroche, S., T. M. Jay, et al. (1990). "Long-term potentiation in the prefrontal cortex following stimulation of the hippocampal CA1/subicular region." Neurosci Lett **114**(2): 184-190.

Lavin, A. and A. A. Grace (1998). "Dopamine modulates the responsivity of mediodorsal thalamic cells recorded in vitro." J Neurosci **18**(24): 10566-10578.

Lee, I. and R. P. Kesner (2003). "Time-dependent relationship between the dorsal hippocampus and the prefrontal cortex in spatial memory." J Neurosci **23**(4): 1517-1523.

Li, S., W. Bai, et al. (2012). "Increases of theta-low gamma coupling in rat medial prefrontal cortex during working memory task." Brain Res Bull **89**(3-4): 115-123.

Liddle, P. F. (2000). "Cognitive impairment in schizophrenia: its impact on social functioning." Acta Psychiatr Scand Suppl **400**: 11-16.

Linden, D. E. (2007). "The working memory networks of the human brain." Neuroscientist **13**(3): 257-267.

Loffler, S., J. Korber, et al. (2012). "Comment on "Impaired respiratory and body temperature control upon acute serotonergic neuron inhibition"." Science **337**(6095): 646; author reply 646.

Loureiro, M., T. Cholvin, et al. (2012). "The ventral midline thalamus (reuniens and rhomboid nuclei) contributes to the persistence of spatial memory in rats." J Neurosci **32**(29): 9947-9959.

Loureiro, M., L. Lecourtier, et al. (2012). "The ventral hippocampus is necessary for expressing a spatial memory." Brain Struct Funct **217**(1): 93-106.

Luck, D., J. M. Danion, et al. (2010). "Abnormal medial temporal activity for bound information during working memory maintenance in patients with schizophrenia." Hippocampus **20**(8): 936-948.

Mallet, N., A. Pogosyan, et al. (2008). "Parkinsonian beta oscillations in the external globus pallidus and their relationship with subthalamic nucleus activity." J Neurosci **28**(52): 14245-14258.

Mao, J. B. and J. K. Robinson (1998). "Microinjection of GABA-A agonist muscimol into the dorsal but not the ventral hippocampus impairs non-mnemonic measures of delayed non-matching-to-position performance in rats." Brain Res **784**(1-2): 139-147.

Marco-Pallares, J., D. Cucurell, et al. (2008). "Human oscillatory activity associated to reward processing in a gambling task." Neuropsychologia **46**(1): 241-248.

McHugh, S. B., T. G. Campbell, et al. (2008). "A role for dorsal and ventral hippocampus in inter-temporal choice cost-benefit decision making." Behav Neurosci **122**(1): 1-8.

McOmish, C. E., A. Lira, et al. (2012). "Clozapine-induced locomotor suppression is mediated by 5-HT(2A) receptors in the forebrain." Neuropsychopharmacology **37**(13): 2747-2755.

Milner, B. (1982). "Some cognitive effects of frontal-lobe lesions in man." Philos Trans R Soc Lond B Biol Sci **298**(1089): 211-226.

Minzenberg, M. J., A. R. Laird, et al. (2009). "Meta-analysis of 41 functional neuroimaging studies of executive function in schizophrenia." Arch Gen Psychiatry **66**(8): 811-822.

Mitchell, A. S. and J. C. Dalrymple-Alford (2005). "Dissociable memory effects after medial thalamus lesions in the rat." Eur J Neurosci **22**(4): 973-985.

Mitelman, S. A., W. Byne, et al. (2005). "Metabolic disconnection between the mediodorsal nucleus of the thalamus and cortical Brodmann's areas of the left hemisphere in schizophrenia." Am J Psychiatry **162**(9): 1733-1735.

Mongillo, G., O. Barak, et al. (2008). "Synaptic theory of working memory." Science **319**(5869): 1543-1546.

Montgomery, K. C. (1952). "Exploratory behavior and its relation to spontaneous alternation in a series of maze exposures." J Comp Physiol Psychol **45**(1): 50-57.

Montgomery, S. M., M. I. Betancur, et al. (2009). "Behavior-dependent coordination of multiple theta dipoles in the hippocampus." J Neurosci **29**(5): 1381-1394.

Moser, E., M. B. Moser, et al. (1993). "Spatial learning impairment parallels the magnitude of dorsal hippocampal lesions, but is hardly present following ventral lesions." J Neurosci **13**(9): 3916-3925.

Moser, M. B. and E. I. Moser (1998). "Functional differentiation in the hippocampus." Hippocampus **8**(6): 608-619.

Moser, M. B., E. I. Moser, et al. (1995). "Spatial learning with a minislab in the dorsal hippocampus." Proc Natl Acad Sci U S A **92**(21): 9697-9701.

Nambu, A. and R. Llinas (1994). "Electrophysiology of globus pallidus neurons in vitro." J Neurophysiol **72**(3): 1127-1139.

Neave, N., A. Sahgal, et al. (1993). "Lack of effect of dorsomedial thalamic lesions on automated tests of spatial memory in the rat." Behav Brain Res **55**(1): 39-49.

Nini, A., A. Feingold, et al. (1995). "Neurons in the globus pallidus do not show correlated activity in the normal monkey, but phase-locked oscillations appear in the MPTP model of parkinsonism." J Neurophysiol **74**(4): 1800-1805.

Olton, D. S. (1979). "Mazes, maps, and memory." Am Psychol **34**(7): 583-596.

Park, S., P. S. Holzman, et al. (1995). "Spatial working memory deficits in the relatives of schizophrenic patients." Arch Gen Psychiatry **52**(10): 821-828.

Perala, J., J. Suvisaari, et al. (2007). "Lifetime prevalence of psychotic and bipolar I disorders in a general population." Arch Gen Psychiatry **64**(1): 19-28.

Perlstein, W. M., C. S. Carter, et al. (2001). "Relation of prefrontal cortex dysfunction to working memory and symptoms in schizophrenia." Am J Psychiatry **158**(7): 1105-1113.

Petrides, M. (1996). "Specialized systems for the processing of mnemonic information within the primate frontal cortex." Philos Trans R Soc Lond B Biol Sci **351**(1346): 1455-1461; discussion 1461-1452.

Pettersson-Yeo, W., P. Allen, et al. (2011). "Dysconnectivity in schizophrenia: where are we now?" Neurosci Biobehav Rev **35**(5): 1110-1124.

Pitkanen, A., M. Pikkarainen, et al. (2000). "Reciprocal connections between the amygdala and the hippocampal formation, perirhinal cortex, and postrhinal cortex in rat. A review." Ann N Y Acad Sci **911**: 369-391.

Pontecorvo, M. J. (1983). "Effects of proactive interference on rats' continuous nonmatching-to-sample performance." Anim. Learn Behavior **11**: 356-366.

Ray, R. S., A. E. Corcoran, et al. (2011). "Impaired respiratory and body temperature control upon acute serotonergic neuron inhibition." Science **333**(6042): 637-642.

Royer, S., A. Sirota, et al. (2010). "Distinct representations and theta dynamics in dorsal and ventral hippocampus." J Neurosci **30**(5): 1777-1787.

Rygula, R., S. C. Walker, et al. (2010). "Differential contributions of the primate ventrolateral prefrontal and orbitofrontal cortex to serial reversal learning." J Neurosci **30**(43): 14552-14559.

Sarnthein, J., H. Petsche, et al. (1998). "Synchronization between prefrontal and posterior association cortex during human working memory." Proc Natl Acad Sci U S A **95**(12): 7092-7096.

Schmiedt, C., A. Brand, et al. (2005). "Event-related theta oscillations during working memory tasks in patients with schizophrenia and healthy controls." Brain Res Cogn Brain Res **25**(3): 936-947.

Schmitzer-Torbert, N., J. Jackson, et al. (2005). "Quantitative measures of cluster quality for use in extracellular recordings." Neuroscience **131**(1): 1-11.

Schoenbaum, G., S. L. Nugent, et al. (2002). "Orbitofrontal lesions in rats impair reversal but not acquisition of go, no-go odor discriminations." Neuroreport **13**(6): 885-890.

Seidenbecher, T., T. R. Laxmi, et al. (2003). "Amygdalar and hippocampal theta rhythm synchronization during fear memory retrieval." Science **301**(5634): 846-850.

Seidman, L. J., D. Yurgelun-Todd, et al. (1994). "Relationship of prefrontal and temporal lobe MRI measures to neuropsychological performance in chronic schizophrenia." Biol Psychiatry **35**(4): 235-246.

Sesack, S. R., A. Y. Deutch, et al. (1989). "Topographical organization of the efferent projections of the medial prefrontal cortex in the rat: an anterograde tract-tracing study with Phaseolus vulgaris leucoagglutinin." J Comp Neurol **290**(2): 213-242.

Shi, C. J. and M. D. Cassell (1999). "Perirhinal cortex projections to the amygdaloid complex and hippocampal formation in the rat." J Comp Neurol **406**(3): 299-328.

Siapas, A. G., E. V. Lubenov, et al. (2005). "Prefrontal phase locking to hippocampal theta oscillations." Neuron **46**(1): 141-151.

Siegel, M., M. R. Warden, et al. (2009). "Phase-dependent neuronal coding of objects in short-term memory." Proc Natl Acad Sci U S A **106**(50): 21341-21346.

Sigurdsson, T., K. L. Stark, et al. (2010). "Impaired hippocampal-prefrontal synchrony in a genetic mouse model of schizophrenia." Nature **464**(7289): 763-767.

Silver, H., P. Feldman, et al. (2003). "Working memory deficit as a core neuropsychological dysfunction in schizophrenia." Am J Psychiatry **160**(10): 1809-1816.

Simpson, E. H., C. Kellendonk, et al. (2010). "A possible role for the striatum in the pathogenesis of the cognitive symptoms of schizophrenia." Neuron **65**(5): 585-596.

Singer, W. (1999). "Neuronal synchrony: a versatile code for the definition of relations?" Neuron **24**(1): 49-65, 111-125.

Sirota, A., S. Montgomery, et al. (2008). "Entrainment of neocortical neurons and gamma oscillations by the hippocampal theta rhythm." Neuron **60**(4): 683-697.

Stanford, I. M. (2003). "Independent neuronal oscillators of the rat globus pallidus." J Neurophysiol **89**(3): 1713-1717.

Stokes, K. A. and P. J. Best (1990). "Response biases do not underlie the radial maze deficit in rats with mediodorsal thalamus lesions." Behav Neural Biol **53**(3): 334-345.

Tallon-Baudry, C., O. Bertrand, et al. (2001). "Oscillatory synchrony between human extrastriate areas during visual short-term memory maintenance." J Neurosci **21**(20): RC177.

Tallon-Baudry, C., S. Mandon, et al. (2004). "Oscillatory synchrony in the monkey temporal lobe correlates with performance in a visual short-term memory task." Cereb Cortex **14**(7): 713-720.

Tesche, C. D. and J. Karhu (2000). "Theta oscillations index human hippocampal activation during a working memory task." Proc Natl Acad Sci U S A **97**(2): 919-924.

Tierney, P. L., E. Degenetais, et al. (2004). "Influence of the hippocampus on interneurons of the rat prefrontal cortex." Eur J Neurosci **20**(2): 514-524.

Tolman, E. C. (1925). "Purpose and cognition: the determiners of animal learning." Psychol Rev **32**: 285-297.

Tort, A. B., R. W. Komorowski, et al. (2009). "Theta-gamma coupling increases during the learning of item-context associations." Proc Natl Acad Sci U S A **106**(49): 20942-20947.

Uhlhaas, P. J. and W. Singer (2010). "Abnormal neural oscillations and synchrony in schizophrenia." Nat Rev Neurosci **11**(2): 100-113.

Van der Werf, Y. D., M. P. Witter, et al. (2002). "The intralaminar and midline nuclei of the thalamus. Anatomical and functional evidence for participation in processes of arousal and awareness." Brain Res Brain Res Rev **39**(2-3): 107-140.

Vanderwolf, C. H. (1969). "Hippocampal electrical activity and voluntary movement in the rat." Electroencephalogr Clin Neurophysiol **26**(4): 407-418.

Varela, C., S. Kumar, et al. (2013). "Anatomical substrates for direct interactions between hippocampus, medial prefrontal cortex, and the thalamic nucleus reuniens." Brain Struct Funct.

Varela, F., J. P. Lachaux, et al. (2001). "The brainweb: phase synchronization and large-scale integration." Nat Rev Neurosci **2**(4): 229-239.

Vertes, R. P. (2006). "Interactions among the medial prefrontal cortex, hippocampus and midline thalamus in emotional and cognitive processing in the rat." Neuroscience **142**(1): 1-20.

Vertes, R. P., W. B. Hoover, et al. (2006). "Efferent projections of reuniens and rhomboid nuclei of the thalamus in the rat." J Comp Neurol **499**(5): 768-796.

Wang, G. W. and J. X. Cai (2006). "Disconnection of the hippocampal-prefrontal cortical circuits impairs spatial working memory performance in rats." Behav Brain Res **175**(2): 329-336.

Wang, G. W. and J. X. Cai (2008). "Reversible disconnection of the hippocampal-prelimbic cortical circuit impairs spatial learning but not passive avoidance learning in rats." Neurobiol Learn Mem **90**(2): 365-373.

Watanabe, Y. and S. Funahashi (2012). "Thalamic mediodorsal nucleus and working memory." Neurosci Biobehav Rev **36**(1): 134-142.

Weinberger, D. R. and K. F. Berman (1996). "Prefrontal function in schizophrenia: confounds and controversies." Philos Trans R Soc Lond B Biol Sci **351**(1346): 1495-1503.

Weinberger, D. R., K. F. Berman, et al. (1986). "Physiologic dysfunction of dorsolateral prefrontal cortex in schizophrenia. I. Regional cerebral blood flow evidence." Arch Gen Psychiatry **43**(2): 114-124.

Wilson, M. A. and B. L. McNaughton (1993). "Dynamics of the hippocampal ensemble code for space." Science **261**(5124): 1055-1058.

Witter, M. P., Amaral, D.G. (2004). Hippocampal formation. The rat nervous system. P. G. San Diego, CA, Elsevier Academic Press**:** 635-704.

Yoon, T., J. Okada, et al. (2008). "Prefrontal cortex and hippocampus subserve different components of working memory in rats." Learn Mem **15**(3): 97-105.